Available online at http://scik.org
Commun. Math. Biol. Neurosci. 2021, 2021:31
https://doi.org/10.28919/cmbn/4954
ISSN: 2052-2541

ON THE OPTIMAL VACCINATION AND TRAVEL-RESTRICTION CONTROLS WITH A DISCRETE MULTI-REGION SIRS EPIDEMIC MODEL

HAMZA BOUTAYEB[1,*], SARA BIDAH[1] , OMAR ZAKARY[1] , MUSTAPHA LHOUS[2], MOSTAFA RACHIK[1]

[1]Laboratory of Analysis, Modeling and Simulation (LAMS), Department of Mathematics and Computer Science, Hassan II University of Casablanca, Faculty of Sciences Ben M'Sik, Sidi Othman, BP 7955, Casablanca, Morocco

[2]Department of Mathematics and Computer Science, Faculty of Sciences Ain Chock, University Hassan II Casablanca, Casablanca, Morocco

Copyright © 2021 the author(s). This is an open access article distributed under the Creative Commons Attribution License, which permits unrestricted use, distribution, and reproduction in any medium, provided the original work is properly cited.

Abstract. Pandemics have shaped human history and they remain with us today. Recognizing how these diseases spread can therefore help identify specific disease control strategies. Classical mathematical models describing the evolution of infectious diseases underestimate the effect of the spatio-temporal spread of epidemics. Currently, the COVID-19 pandemic shows the importance of taking into account the spatial dynamics of epidemics and pandemics and the need for new control strategies including vaccinations, awareness and travel restrictions. Here, we consider a SIRS discrete-time multi-regional epidemic model that describes the spatial spread of an epidemic in different geographic areas believed to be related to movements of their populations. We propose a novel approach of optimal control by defining new functions of importance to identify affected areas based on infection thresholds that determine whether the need for a control intervention or not. Numerical results are provided to illustrate our results by applying this new approach in adjacent areas of Morocco, that is, the Casablanca-Settat regions. We study different scenarios to show the most efficient scenario, based on the threshold values.

Keywords: importance functions; automated optimal control; multi-region SIRS model; vaccination; travel-restriction.

*Corresponding author

E-mail address: hz.bouty@gmail.com

Received August 17, 2020

2010 AMS Subject Classification: 39A05, 39A45, 39A60, 93C35, 93C55.

1. INTRODUCTION

Mathematics has been intertwined with every major discipline in the biological and biomedical sciences including epidemiology [1, 2]. Until the twentieth century, epidemiological studies were mostly concerned with infectious diseases [3]; the mathematical epidemiology aimed for describing the transmission process of an epidemic and providing a further understanding of the mechanisms of disease transmission and spread [4]. Mathematical modeling of epidemics provides an estimate for the potential scale of an epidemic, and helps to pinpoint key factors in the disease transmission process, then recommend effective control and preventive measures [5]. Furthermore, it is useful in building and testing theories, and in comparing, planning, implementing and evaluating various detection, prevention, and control programs [6]. Now models of disease transmission are recognized as a valuable tool, they are being integrated into the public health decision-making process more than ever before [7]. But the real impact of mathematical modeling on public health came with the need for evaluating intervention strategies for newly emerging and re-emerging pathogens. Epidemiological modeling present a practical tool for analyzing the process of an epidemic within difined population and taking into consideration the factor of variation in the geographic areas [8].

The process of an epidemic model consist of two major factors; first is a defined population, and second is an exposure to infectious material. The simplest model SIR (Susceptible, Infectious, and Recovered) model was originated in the early 20th century. The members of the population are related to one of three basic classes: Susceptibles (people who may become infectives when making contact with the infectious material). Infectives (reacting as hosts to the infectious material). Removals (Those who have been eliminated for some reason such as death, immunity, hospitalization..). The idea of this process may be described, as one transformation from (susceptible) to another (infective) due to the exposure to some phenomenon. This model's aim is to understand how an epidemic spreads besides the total number infected, or the duration of an infectious disease, in addition to this SIR model can show how different public health interventions could influence the outcome of the epidemic [9, 10]

Mathematical modeling has played important role in describing and analyzing the evolution of an epidemic [8], besides the fact of controlling many contagious diseases such as Smallpox [11], SARS [12], AIDS [13], Tuberculosis [14], Cholera [15], Measles [16], Malaria [17] among other different kinds of contagious diseases..

Epidemics have shaped human history and they remain with us today. Recognizing how these diseases spread can contribute consequently to identifying accurate disease control strategies [18]. A crucial component of this knowledge is the pattern of disease spread in time and space as the disease could be spatially mobile from one region to another [8]. For example the new Coronavirus spreads across mainland China and elsewhere around the globe and sometimes, outbreaks spread over large areas, and can even reach continents. Such cases include the Black Death plague, measles and smallpox, HIV/AIDS, and SARS [19].

In [8] a discrete-time SIR model is presented and devised in various geographical regions to control the spatio-temporal propagation of an epidemic, in this model infected people have the ability to spread the disease from one region to another via travel. The multi-regional discrete-time SIR model focuses on the intervention of multiple regions, in contrast to other models that have mainly focused on the optimization of one single region. This presentation could help managing the issue of regional spread of an infectious disease by organizing many strategies such as vaccination campaigns in order to decrease the number of infected people, or travel-restriction blocking movement of people coming from borders of infected regions. The authors use a finite-dimensional models to analyse the spatio-temporal spread of epidemics as another option of the partial derivatives models.

In this paper, we propose a new optimal control approach mainly based on a multi-regions discrete-time model and a new form of multi-objective optimization criteria with importance functions and which is subject to multi-points boundary value optimal control problems. In this work, with more clarifications and essential details, we devise a multi-regions discrete model for the study of the spread of an epidemic in M different zones and we analyze the effectiveness of vaccination (or awareness) and travel-restriction optimal control strategies when vaccination campaigns and/or travel restriction are applied in infected zones based on the number of infections. Also, we study the case when controls are applied to people who belong to all those regions and

who are supposed to be reachable for every agent (nurse, doctor or media). This last one is responsible for the accomplishment of control strategies followed against the disease.

We consider an area as an infected zone if its number of infected individuals exceeds a threshold defined by the health decision-makers. Therefore, varying the values of this threshold and simulating the infection situation for different values of these thresholds shows that it is necessary to think about reducing the time between the first infection and the implementation of the control strategy. Unexpected results that in some situations the neighboring regions infected and its number of infections exceeds the threshold before the number of infections of the region source. This makes the implementation of the travel-restriction control strategy more important.

In our modeling approach, we divide the studied area Ω into different zones that we call cells (or regions). A cell $C_j \in \Omega$ can represent a city, a country or a larger domain. These cells are supposed to be connected by movements of their populations within the domain Ω. We define also a neighboring cells C_k of the cell C_j all zones connected with C_j via every transport mean, thus a cell $C_j \in \Omega$ can have more than one neighboring cell. Here, we suppose that a cell can be infected due to movements of infected people which enter from its neighboring zones.

We carry out the map of the studied area. Then we use different threshold values in the controlled multi-region SIRS model to simulate the epidemic spread within the Casablanca-Settat region illustrated in the Fig.1, by combining the ArcGIS and Matlab programs.

The paper is organized as follows: In Section 2, we give the proposed discrete-time multi-region SIRS epidemic system. In Section 3, we announce theorems of the existence and characterization of the sought optimal controls functions related to the optimal control approach. In Section 4, we provide simulations of the numerical results applied to the Casablanca-Settat region as domain of interest. Finally, we give a conclusion in the last Section.

FIGURE 1. The geographical studied zone Ω: (a) Discretization on region Casablanca-Settat . (b) Discretization of the region on provinces with numbers.

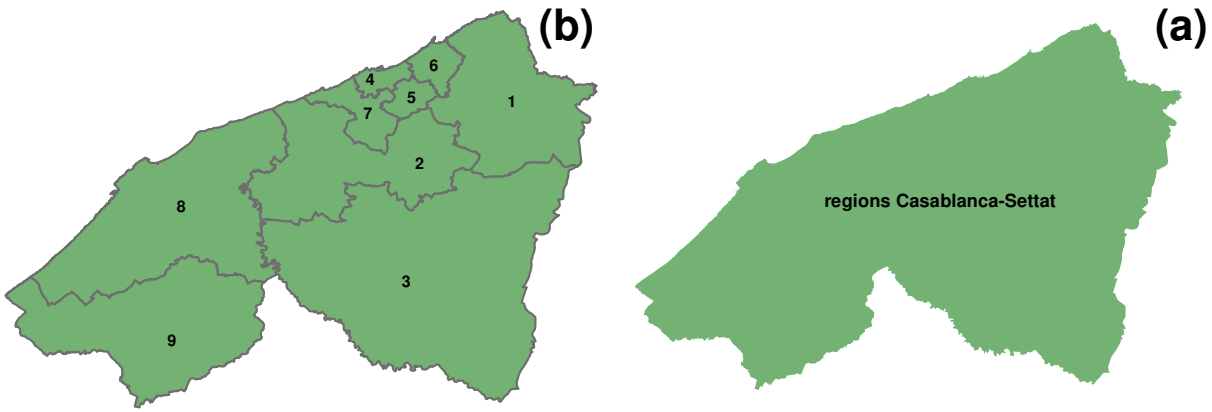

2. MODEL DESCRIPTION AND DEFINITIONS

In this section, Based on modeling assumptions of the reference [8], we consider M geographical zones denoted C_j (sub-domains, regions, cities, towns ...) of the studied domain Ω

$$\Omega = \bigcup_{j=1}^{M} C_j$$

where C_j can represent a city, a country or a larger domain. For instance, the Fig.1 shows an example of geographical discretization of tow regions of Morocco, that is, the nine zones of Casablanca-Settat. We define $V(C_j)$, the vicinity set, composed by all neighboring cells of C_j given by

$$V(C_j) = \left\{ C_k \in \Omega \ / \ C_j \cap C_k \neq \emptyset \right\}, C_j \notin V\left(C_j\right)$$

where $C_j \cap C_k \neq \emptyset$ means that there exists at least one mean of transport between C_j and C_k. Note that this definition of $V(C_j)$ is more general where it defines a more general form of vicinity regardless the geographical location of zones.

Nb	Zone	Population	Nb	Zone	Population	Nb	Zone	Population
1	BEN SLIMANE	233123	4	Casablanca	3359818	7	Nouaceur	333604
2	Berrechid	484518	5	Mediouna	172680	8	El Jadida	786716
3	Settat	634184	6	Mohammadia	404648	9	Sidi Bennour	452448

TABLE 1. Populations of the regions Casablanca-Settat Fig.1.

The multi-regional discrete-time SIRS model associated to C_j when there is no control introduced yet is then

$$S_{i+1}^{C_j} = S_i^{C_j} - \beta_{jj}\frac{I_i^{C_j}}{N_i^{C_j}}S_i^{C_j} - \sum_{C_k \in V(C_j)} \beta_{jk}\frac{I_i^{C_k}}{N_i^{C_j}}S_i^{C_j} + \left(N_i^{C_j} - S_i^{C_j}\right)d_j + \theta_j R_i^{C_j} \tag{1}$$

$$I_{i+1}^{C_j} = I_i^{C_j} + \beta_{jj}\frac{I_i^{C_j}}{N_i^{C_j}}S_i^{C_j} + \sum_{C_k \in V(C_j)} \beta_{jk}\frac{I_i^{C_k}}{N_i^{C_j}}S_i^{C_j} - \gamma_j I_i^{C_j} - d_j I_i^{C_j} - \alpha_j I_i^{C_j} \tag{2}$$

$$R_{i+1}^{C_j} = R_i^{C_j} + \gamma_j I_i^{C_j} - d_j R_i^{C_j} - \theta_j R_i^{C_j} \tag{3}$$

where the disease transmission coefficient $\beta_{jk} > 0$ is the proportion of adequate contacts in domain C_j between a susceptible from C_j $(j = 1, ..., M)$ and an infective from another domain C_k. The coefficient d_j is the birth and death rate. The parameter γ_j is is the recovery rate. The coefficient α_j is the proportion of mortality due to the disease. The biological background requires that all parameters be non-negative. The parameter θ_j is the proportion that a recovered becomes again a susceptible. The notations $S_i^{C_j}, I_i^{C_j}$ and $R_i^{C_j}$ represent the numbers of individuals in the susceptible, infective and recovered compartments of C_j at time i, respectively. The population size corresponding to domain C_j at time i is given by $N_i^{C_j} = S_i^{C_j} + I_i^{C_j} + R_i^{C_j}$. It is clear that the population size is not constant for all $i \geq 0$.

3. TRAVEL-RESTRICTION AND VACCINATION CONTROLS

3.1. Presentation of the model with controls. In this section, we introduce a control variable $u_i^{C_j}$ that characterizes the effectiveness of the vaccination in the above mentioned model (1-3). This control in some situations can represent the effect of the awareness and media programs [19, 20].

In almost all infectious diseases, the authorities determine the threshold of risk based on many factors, such as availability of medical equipment, budgets, and medical personnel ... Thus, they can wait some time to see the course of events before the intervention. If the number of casualties exceeds a predefined limit, decision-makers have no choice but to start trying to control the situation. This motivate us to define a Boolean function $\varepsilon_i^{C_j}$ ($\varepsilon_i^{C_j} = 1$ or $\varepsilon_i^{C_j} = 0$) associated to the domain C_j, that will be called the importance function of C_j. Where $\varepsilon_i^{C_j}$ is either equaling to 1, in the case when the number of infections in the cell C_j at instant i is greater than or equal to the threshold of vaccination $\mathscr{I}_V^{C_j}$ defined by the authorities and health decision-makers, or $\varepsilon_i^{C_j} = 0$ otherwise. Therefore, we define the importance function associated to the vaccination control $\varepsilon_{v,i}^{C_j}$ by the Heaviside step function H as follows

$$\varepsilon_{v,i}^{C_j} = H\left(I_i^{C_j} - \mathscr{I}^{C_j}\right) = \begin{cases} 0 & I_i^{C_j} < \mathscr{I}_V^{C_j} \\ 1 & I_i^{C_j} \geq \mathscr{I}_V^{C_j} \end{cases}$$

In the case of epidemics and pandemics, and in the absence of effective treatment, governments tend to take non-drug measures to reduce the number of victims. Travel restrictions, self-isolation and social isolation are the most commonly used non-drug measures in such situations. Therefore, we introduce a second control variable $v_i^{C_j}$ that characterizes the travel-restriction operation which aims to restrict movements of people coming from neighboring zones $C_k \in V(C_j)$ to the affected zone C_j, in order to facilitate the categorization of people depending on their cases. Thus, we define a threshold based on the number of infections to determine affected zones. Then, $\mathscr{I}_T^{C_j}$ is the tolerable number of infections in the zone C_j before the closure of this zone, i.e. if the number of infections $I_i^{C_j}$ in C_j exceeds $\mathscr{I}_T^{C_j}$, C_j is called an affected zone and then the travel-restriction will be applied. Therefore, the importance function associated to the travel-restriction control $\varepsilon_{T,i}^{C_j}$ is also defined by the Heaviside step function H as follows

$$\varepsilon_{T,i}^{C_j} = H\left(I_i^{C_j} - I_{sT}^{C_j}\right) = \begin{cases} 0 & I_i^{C_j} < \mathscr{I}_T^{C_j} \\ 1 & I_i^{C_j} \geq \mathscr{I}_T^{C_j} \end{cases}$$

Based on all these considerations, for a given zone $C_j \in \Omega$, the model is given by the following equations

$$
\begin{aligned}
S_{i+1}^{C_j} &= S_i^{C_j} - \beta_{jj}\frac{I_i^{C_j}}{N_i^{C_j}}S_i^{C_j} - \sum_{C_k \in V(C_j)} \left(1 - \varepsilon_{T,i}^{C_j} v_i^{C_j}\right) \beta_{jk}\frac{I_i^{C_k}}{N_i^{C_j}}S_i^{C_j} \\
&\quad + \left(N_i^{C_j} - S_i^{C_j}\right) d_j + \theta_j R_i^{C_j} - \varepsilon_{v,i}^{C_j} u_i^{C_j} S_i^{C_j} \qquad (4)
\end{aligned}
$$

$$
\begin{aligned}
I_{i+1}^{C_j} &= I_i^{C_j} + \beta_{jj}\frac{I_i^{C_j}}{N_i^{C_j}}S_i^{C_j} + \sum_{C_k \in V(C_j)} \left(1 - \varepsilon_{T,i}^{C_j} v_i^{C_j}\right) \beta_{jk}\frac{I_i^{C_k}}{N_i^{C_j}}S_i^{C_j} \\
&\quad - \gamma_j I_i^{C_j} - d_j I_i^{C_j} - \alpha_j I_i^{C_j} \qquad (5)
\end{aligned}
$$

$$
R_{i+1}^{C_j} = R_i^{C_j} + \gamma_j I_i^{C_j} - d_j R_i^{C_j} - \theta_j R_i^{C_j} + \varepsilon_{v,i}^{C_j} u_i^{C_j} S_i^{C_j} \qquad (6)
$$

Our goal is obviously to try to minimize the population of the susceptible and infected groups and the cost of vaccinations and travel-restriction in all affected zones.

3.2. An optimal control approach. We devise in this paper an automated optimal control approach for each region with different importance functions $\varepsilon_{*,i}^{C_j}$, $j = 1, ..., M$. We characterize optimal controls that minimize the number of the infected people and maximize the ones in the recovered category for all affected regions. Then, we are interested by minimizing the functional

$$
J(u, v) = \sum_{k=1}^{M} max\left(\varepsilon_{v,i}^{C_j}, \varepsilon_{T,i}^{C_j}\right) J_k\left(u^{C_k}, v^{C_k}\right) \qquad (7)
$$

where $J_j(u^{C_k}, v^{C_k})$ is given by

$$
J_j(u^{C_j}, v^{C_j}) = \left(\alpha_j^I I_N^{C_j} - \alpha_j^R R_N^{C_j}\right) + \sum_{i=1}^{N-1} \left[\alpha_j^I I_i^{C_j} - \alpha_j^R R_i^{C_j} + \varepsilon_{v,i}^{C_j}\frac{A_j}{2}\left(u_i^{C_j}\right)^2 + \varepsilon_{T,i}^{C_j}\frac{B_j}{2}\left(v_i^{C_j}\right)^2\right] \qquad (8)
$$

where $A_j > 0, B_j > 0$, $\alpha_I^{C_j} > 0$, $\alpha_R^{C_j} > 0$ are the weight constants of controls, the infected and the recovered populations in the region C_j respectively, and $u = \left(u^{C_1}, ..., u^{C_M}\right)$ with $u^{C_j} = \left(u_0^{C_j}, ..., u_{N-1}^{C_j}\right)$, and $v = \left(v^{C_1}, ..., v^{C_M}\right)$ with $v^{C_j} = \left(v_0^{C_j}, ..., v_{N-1}^{C_j}\right)$.

Our goal is to minimize the infected individuals, minimize the systemic costs of vaccinations and travel-restriction attempting to increase the number of recovered people in each zone $C_j \in \Omega$. In other words, we are seeking optimal controls u^* and v^* such that

$$
J(u^*, v^*) = min\{J(u, v) / u \in U, v \in V\}
$$

where U and V are the control sets defined by

$$U = \left\{ u \,\text{measurable} / u_{min}^{C_j} \leq u_i^{C_j} \leq u_{max}^{C_j},\, i = 0,...,N-1,\, j = 1,...,M \right\} \tag{9}$$

$$V = \left\{ v \,\text{measurable} / v_{min}^{C_j} \leq v_i^{C_j} \leq v_{max}^{C_j},\, i = 0,...,N-1,\, j = 1,...,M \right\} \tag{10}$$

where $0 < u_{min}^{C_j} < u_{max}^{C_j} < 1$ and $0 < v_{min}^{C_j} < v_{max}^{C_j} < 1$, by using Pontryagin's Maximum Principle [21] we derive necessary conditions for our optimal controls. For this purpose we define the Hamiltonian as

$$\begin{aligned}
\mathscr{H} \quad = \quad & \sum_{k=1}^{M} max(\varepsilon_{v,i}^{C_k}, \varepsilon_{T,i}^{C_k}) \left[\alpha_k^I I_i^{C_k} - \alpha_k^R R_i^{C_k} + \varepsilon_{v,i}^{C_k} \frac{A_k}{2} \left(u_i^{C_k} \right)^2 + \varepsilon_{T,i}^{C_k} \frac{B_k}{2} (v_i^{C_k})^2 \right] \\
& + \sum_{j=1}^{M} max(\varepsilon_{v,i}^{C_j}, \varepsilon_{T,i}^{C_j}) \left(\zeta_{1,i+1}^j \left[S_i^{C_j} - \beta_{jj} \frac{I_i^{C_j}}{N_i^{C_j}} S_i^{C_j} - \sum_{C_k \in V(C_j)} \left(1 - \varepsilon_{T,i}^{C_j} v_i^{C_j} \right) \beta_{jk} \frac{I_i^{C_k}}{N_i^{C_j}} S_i^{C_j} \right. \right. \\
& \left. + \left(N_i^{C_j} - S_i^{C_j} \right) d_j + \theta_j R_i^{C_j} - \varepsilon_{v,i}^{C_j} u_i^{C_j} S_i^{C_j} \right] \\
& + \zeta_{2,i+1}^j \left[I_i^{C_j} + \beta_{jj} \frac{I_i^{C_j}}{N_i^{C_j}} S_i^{C_j} + \sum_{C_k \in V(C_j)} \left(1 - \varepsilon_{T,i}^{C_j} v_i^{C_j} \right) \beta_{jk} \frac{I_i^{C_k}}{N_i^{C_j}} S_i^{C_j} \right. \\
& \left. - \gamma_j I_i^{C_j} - d_j I_i^{C_j} - \alpha_j I_i^{C_j} \right] \\
& + \left. \zeta_{3,i+1}^j \left[R_i^{C_j} + \gamma_j I_i^{C_j} - d_j R_i^{C_j} - \theta_j R_i^{C_j} + \varepsilon_{v,i}^{C_j} u_i^{C_j} S_i^{C_j} \right] \right)
\end{aligned} \tag{11}$$

Theorem 1. *Given optimal controls $u^{C_j *}$, $v^{C_j *}$ and solutions $S^{C_j *}, I^{C_j *}$ and $R^{C_j *}$, there exists $\zeta_{k,i}^j$, $i = 1,...,N$, $k = 1,2,3$, the adjoint variables satisfying the following equations*

$$\begin{aligned}
\Delta \zeta_{1,i}^j \quad = \quad & -max(\varepsilon_{v,i}^{C_j}, \varepsilon_{T,i}^{C_j}) \left[\left(1 - \beta_{jj} \frac{I_i^{C_j}}{N_i^{C_j}} - \sum_{C_k \in V(C_j)} \left(1 - \varepsilon_{T,i}^{C_j} v_i^{C_j} \right) \beta_{jk} \frac{I_i^{C_k}}{N_i^{C_j}} - d_j - \varepsilon_{v,i}^{C_j} u_i^{C_j} \right) \zeta_{1,i+1}^j \right. \\
& \left. + \left(\beta_{jj} \frac{I_i^{C_j}}{N_i^{C_j}} + \sum_{C_k \in V(C_j)} \left(1 - \varepsilon_{T,i}^{C_j} v_i^{C_j} \right) \beta_{jk} \frac{I_i^{C_k}}{N_i^{C_j}} \right) \zeta_{2,i+1}^j + \varepsilon_{v,i}^{C_j} u_i^{C_j} \zeta_{3,i+1}^j \right]
\end{aligned} \tag{12}$$

$$\begin{aligned}
\Delta \zeta_{2,i}^j \quad = \quad & -max(\varepsilon_{v,i}^{C_j}, \varepsilon_{T,i}^{C_j}) \left[\alpha_j^I + \beta_{jj} \frac{S_i^{C_j}}{N_i^{C_j}} \left(\zeta_{2,i+1}^j - \zeta_{1,i+1}^j \right) \right. \\
& \left. + \left(1 - \gamma_j - d_j - \alpha_j \right) \zeta_{2,i+1}^j + \gamma_j \zeta_{3,i+1}^j \right]
\end{aligned} \tag{13}$$

$$\Delta \zeta_{3,i}^j = -max(\varepsilon_{v,i}^{C_j}, \varepsilon_{T,i}^{C_j}) \left[-\alpha_j^R + \left(1 - d_j - \theta_j \right) \zeta_{3,i+1}^j + \zeta_{1,i+1}^j \theta_j \right] \tag{14}$$

where $\zeta^j_{1,N}=0, \zeta^j_{2,N}=max\left(\varepsilon^{C_j}_{v,i},\varepsilon^{C_j}_{T,i}\right)\alpha^I_j, \zeta^j_{3,N}=-max\left(\varepsilon^{C_j}_{v,i},\varepsilon^{C_j}_{T,i}\right)\alpha^R_j$ *are the transversality conditions. In addition*

$$u^*=\left(u^{C_1*},...,u^{C_p*}\right) \text{ and } v^*=\left(v^{C_M*},...,u^{C_M*}\right)$$

where $u^{C_j*}=\left(u^{C_j*}_0,...,u^{C_j*}_{N-1}\right)$ *and* $v^{C_j*}=\left(v^{C_j*}_0,...,v^{C_j*}_{N-1}\right)$ *are given by*

$$u^{C_j*}_i = min\left\{max\left\{u^{\Omega_j}_{min}, max\left(\varepsilon^{C_j}_{v,i},\varepsilon^{C_j}_{T,i}\right)\frac{\left(\zeta^j_{1,i+1}-\zeta^j_{3,i+1}\right)S^{C_j*}_i}{A_j}\right\}, u^{C_j}_{max}\right\} \text{ if } \varepsilon^{C_j}_{v,i}=1$$

$$u^{C_j*}_i=0, \quad \text{Otherwise} \tag{15}$$

$$v^{C_j*}_i = min\left\{max\left\{v^{C^k_j}_{min}, max(\varepsilon^{C_j}_{v,i},\varepsilon^{C_j}_{T,i})\frac{(\zeta^j_{2,i+1}-\zeta^j_{1,i+1})}{B_j}\sum_{C_k\varepsilon V(C_j)}\beta_{jk}\frac{I^{C_k}_i}{N^{C_j}_i}S^{C_j}_i\right\}, v^{C^k_j}_{max}\right\} \text{ if } \varepsilon^{C_j}_{T,i}=1 \tag{16}$$

$$v^{C_j*}_i = 0, \textit{Otherwise.}$$

Proof. Using Pontryagin's Maximum Principle [21], we obtain the following adjoint equations

$$\begin{aligned}
\Delta\zeta^{C_j}_{1,i} = -\frac{\partial\mathscr{H}}{\partial S^{C_j}_i} = \quad & -max(\varepsilon^{C_j}_{v,i},\varepsilon^{C_j}_{T,i})\left[\left(1-\beta_{jj}\frac{I^{C_j}_i}{N^{C_j}_i}-\sum_{C_k\in V(C_j)}\left(1-\varepsilon^{C_j}_{T,i}v^{C_j}_i\right)\beta_{jk}\frac{I^{C_k}_i}{N^{C_j}_i}-d_j-\varepsilon^{C_j}_{v,i}u^{C_j}_i\right)\zeta^j_{1,i+1}\right.\\
& \left.+\left(\beta_{jj}\frac{I^{C_j}_i}{N^{C_j}_i}+\sum_{C_k\in V(C_j)}\left(1-\varepsilon^{C_j}_{T,i}v^{C_j}_i\right)\beta_{jk}\frac{I^{C_k}_i}{N^{C_j}_i}\right)\zeta^j_{2,i+1}+\varepsilon^{C_j}_{v,i}u^{C_j}_i\zeta^j_{3,i+1}\right]\\
\Delta\zeta^{C_j}_{2,i} = -\frac{\partial\mathscr{H}}{\partial I^{C_j}_i} = \quad & -max\left(\varepsilon^{C_j}_{v,i},\varepsilon^{C_j}_{T,i}\right)\left[\alpha^I_j+\beta_{jj}\frac{S^{C_j}_i}{N^{C_j}_i}\left(\zeta^j_{2,i+1}-\zeta^j_{1,i+1}\right)+(1-\gamma_j-d_j-\alpha_j)\zeta^j_{2,i+1}+\gamma_j\zeta^j_{3,i+1}\right]\\
\Delta\zeta^{C_j}_{3,i} = -\frac{\partial\mathscr{H}}{\partial R^{C_j}_i} = \quad & -max\left(\varepsilon^{C_j}_{v,i},\varepsilon^{C_j}_{T,i}\right)\left[-\alpha^R_j+(1-d_j-\theta_j)\zeta^j_{3,i+1}+\zeta^j_{1,i+1}\theta_j\right]
\end{aligned}$$

with $\zeta^{C_j}_{1,N}=0, \zeta^{C_j}_{2,N}=\varepsilon^{C_j}_i\alpha^{C_j}_I, \zeta^{C_j}_{3,N}=-\varepsilon^{C_j}_i\alpha^{C_j}_R$. To obtain the optimality conditions we take the variation with respect to control $u^{C_j}_i$ and $v^{C_j}_i$ and solve for u^{C_j} and v^{C_j} respectively we get

$$u^{C_j*}_i = max\left(\varepsilon^{C_j}_{v,i},\varepsilon^{C_j}_{T,i}\right)\frac{\left(\zeta^j_{1,i+1}-\zeta^j_{3,i+1}\right)S^{C_j*}_i}{A_j}$$

$$v^{C^k_j*}_i = max(\varepsilon^{C_j}_{v,i},\varepsilon^{C_j}_{T,i})\frac{(\zeta^j_{2,i+1}-\zeta^j_{1,i+1})}{B_j}\sum_{C_k\varepsilon V(C_j)}\beta_{jk}\frac{I^{C_k}_i}{N^{C_j}_i}S^{C_j}_i$$

By taking bounds of controls from U and V we get the result. □

Parameter	Description	Value
β	Infection rate	1×10^{-3}
d	Birth and death rate	1×10^{-5}
γ	Recovery rate	1×10^{-5}
α	Death due to the infection	1×10^{-4}
θ	loss of immunity	1×10^{-6}

TABLE 2. Parameters values of β, d, θ, α and γ utilized for the resolution of all multi-regions discrete systems and then leading to simulations obtained from Fig.2 to Fig.31, with the initial populations given in Table 1.

4. NUMERICAL RESULTS

In this section, we present numerical simulations associated to the above mentioned optimal control problem. We write a code in $MATLAB^{TM}$ and simulated our results for several scenarios. The optimality systems is solved based on an iterative discrete scheme that converges following an appropriate test similar the one related to the Forward-Backward Sweep Method (FBSM). The state system with an initial guess is solved forward in time and then the adjoint system is solved backward in time because of the transversality conditions. Afterwards, we update the optimal control values using the values of state and co-state variables obtained at the previous steps. Finally, we execute the previous steps till a tolerance criterion is reached.

4.1. Area of interest. We chose the Casablanca-Settat region as the studied area Ω in this paper because we are convinced that we can find some useful data to support our work. They are the most populated and dynamic regions of Morocco, which contain Casablanca city as the economic and industrial capital of Morocco because with its demographic growth and continuous development of the industrial sector, and the 14 other provinces (see Fig.1), in order to illustrate the objective of our work.

Fig.1 illustrates an example of discrete geographical zones of Casablanca-Settat regions (Morocco) where $M = 9$, this image was originally made based on information from [22].

4.2. Geographical vicinity. A shape-file is a simple, non topological format for storing the geometric location and attribute information of geographic features. Geographic features in a shape-file can be represented by points, lines, or polygons (areas). The workspace containing shape-files may also contain database tables, which can store additional attributes that can be joined to a shape-file's features [23]. ArcMap is a central application used in ArcGIS software, where we can view and explore GIS database for our study area, and where we assign symbols and create map layouts for printing or publication. In this application we can represent geographic information as a set of layers and other elements in a map. Common map elements of a map include the data frame containing the map layers for a given extent [24]. Neighborhood tools create output values for each cell location based on the location value and the values identified in a specified neighborhood [25]. We use this tool to create the neighborhood $V(C_j)$ of each separated zone C_j within the area of interest Ω. For instance

$$V(C_{15}) = \{C_5, C_6, C_7\}$$

Without loss of generality, we set the same infection thresholds for all zones, therefore, hereafter we note $\mathscr{I}_T^{C_j}$ as $\mathscr{I}^{\mathscr{T}}{}_{min}$ and $\mathscr{I}_V^{C_j}$ as $\mathscr{I}^{\mathscr{V}}{}_{min}$.

4.3. Scenario 0: Simulation of the multi-region model without any control. In all the rest geographical figures, we consider four time steps (a) $i = 0$, (b) $i = 40$, (c) $i = 80$ (d) $i = 120$, (e) $i = 160$ and (f) $i = 200$. Dark color represents the highest values. Geographical figures show the transmission of infection between different zones while associated graphs show states' changes over time.

Figures 3. (a), (b), (c), (d), (e) and (f) indicate the number of susceptible people in the 9 regions without any control strategy at the moments $i = 0$, $i = 40$, $i = 80$, $i = 120$,$i = 160$ and $i = 200$ respectively. We see from Fig.2 and 3 that the numbers of susceptible people in all regions, except C_9, are constant until the instant $i = 150$, then it decreases by varying between $3.8\ 10^3$ and $7.7\ 10^4$ person. In regions C_2, C_3 and C_{10} the number of susceptible people is almost constant, but in region C_9 the number is constant until $i = 160$ and then it decreases about 10^4.

Fig.4 and Fig.5 represent the evolution and the geographical distribution of the infected individuals in the different regions without controls.

FIGURE 2. Temporal evolution of susceptible populations without the control strategy.

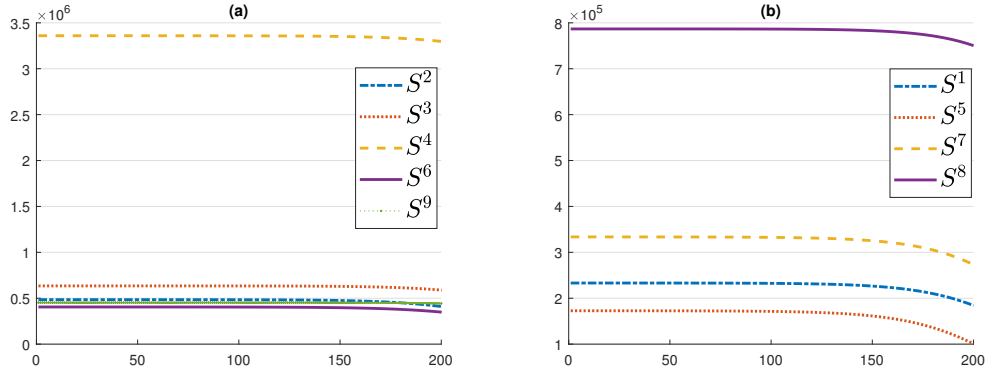

FIGURE 3. Geographical spread of susceptible individuals without the control strategy.

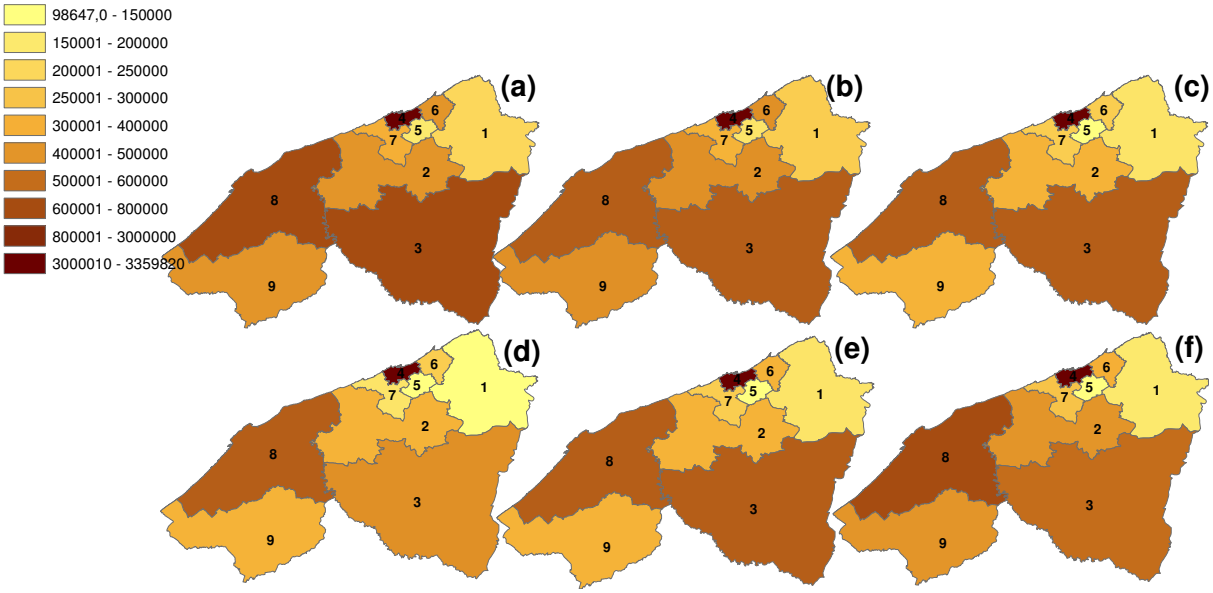

Following Fig.5, at the beginning, all the regions did not record any infection until moment $i = 120$. From the moment $i = 120$, the number of infected increases exponentially. This results is shown clearly in the Fig.4, which has kept the same display in the four first maps (Fig.6(a), (b), (c) and (d)), which means that the number of infected did not exceed 9600 in all regions. In the instant $i = 160$, the region of Casablanca (C_4) and the neighboring regions C_1, C_2, C_5, C_6, C_7 exceeded the 9600 infected. In the final state $i = 200$ we see a strong evolution, all the regions have exceeded 19200 infected except C_9, which has just reached 10^5. The regions C_2 and C_5 have exceeded 67300 infected.

FIGURE 4. Geographical spread of infected individuals without the control strategy.

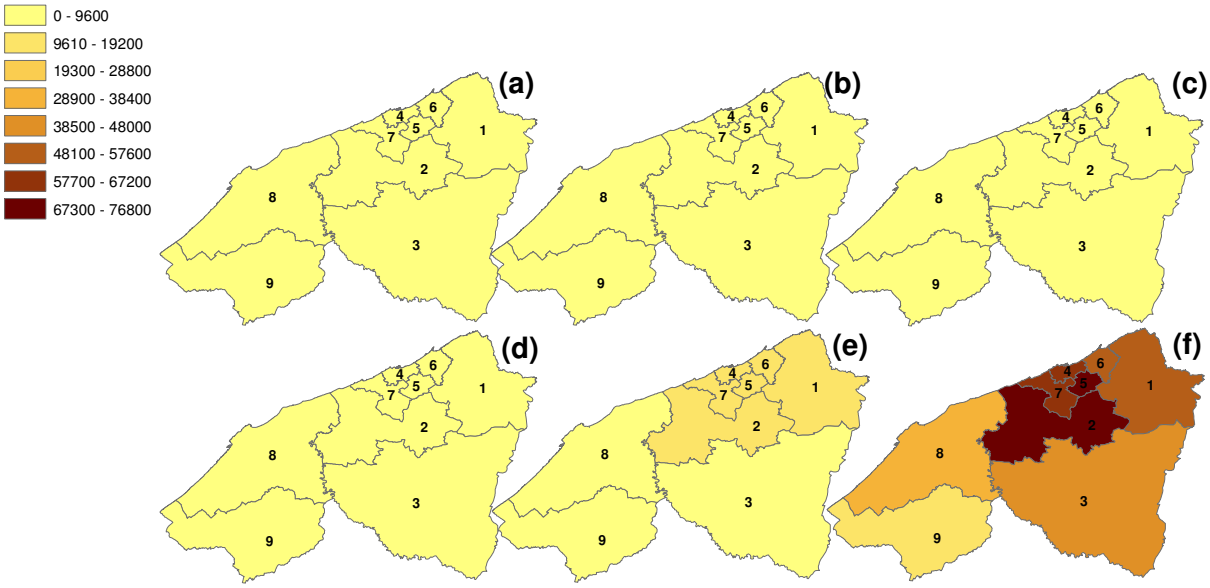

FIGURE 5. Temporal evolution of infected populations without the control strategy.

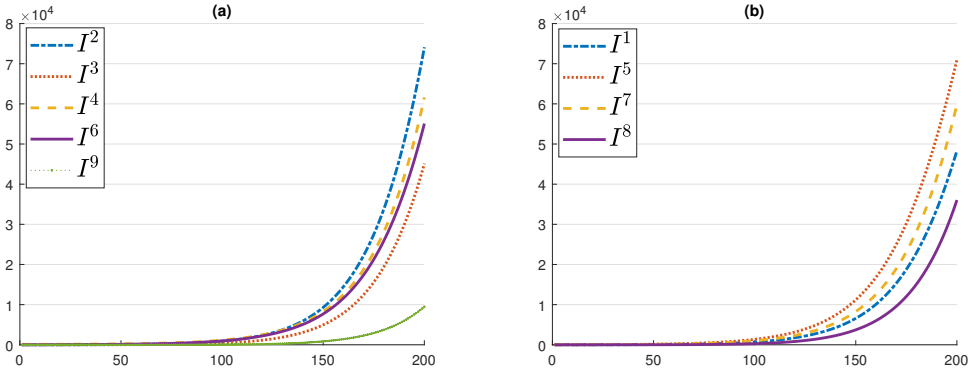

Fig.6 and Fig.7 show the development of the recovered population without controls in the provinces of Casablanca-Settat.

We note that the numbers of the recovered, like the case of the infected, only change from the instant $i = 100$ and gradually increases to reach in the regions C_4, C_6, C_5, C_7 and C_2 that surrounds the city of Casablanca, small values varying between 20 and 40 recovered cases.

In the final state $i = 200$, the C_4 region and its neighboring regions reach values between 130 and 200. In the other regions, that are geographically further from C_4, the number of recovered have do not exceed the 100 cases at the final state.

FIGURE 6. Geographical spread of recovered individuals without the control strategy.

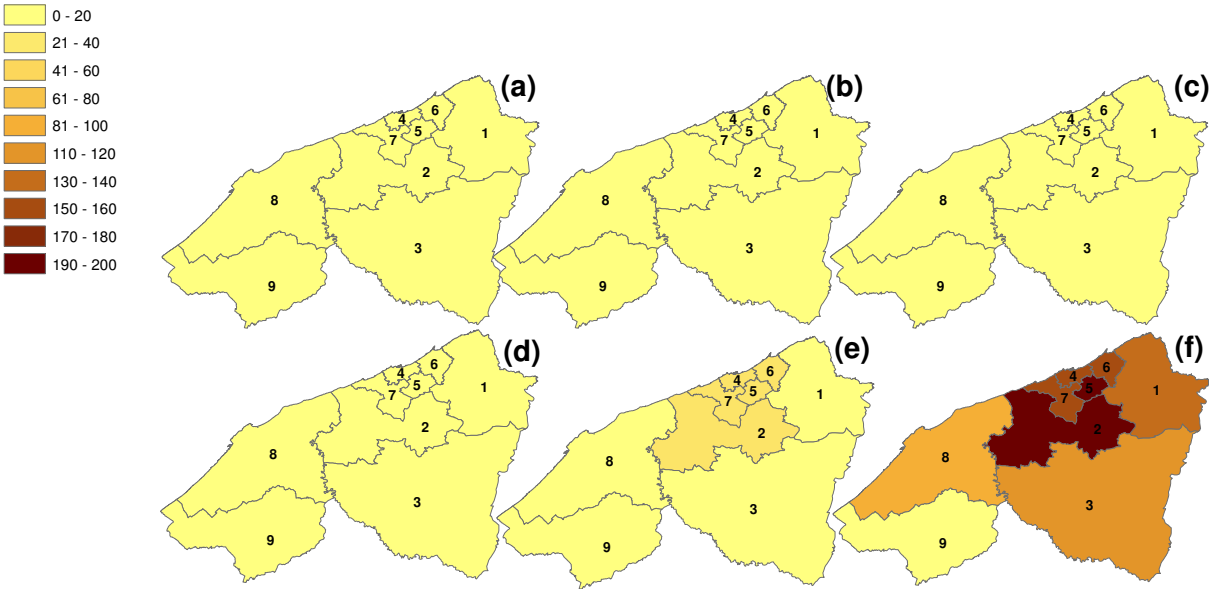

FIGURE 7. Temporal evolution of recovered populations without the control strategy.

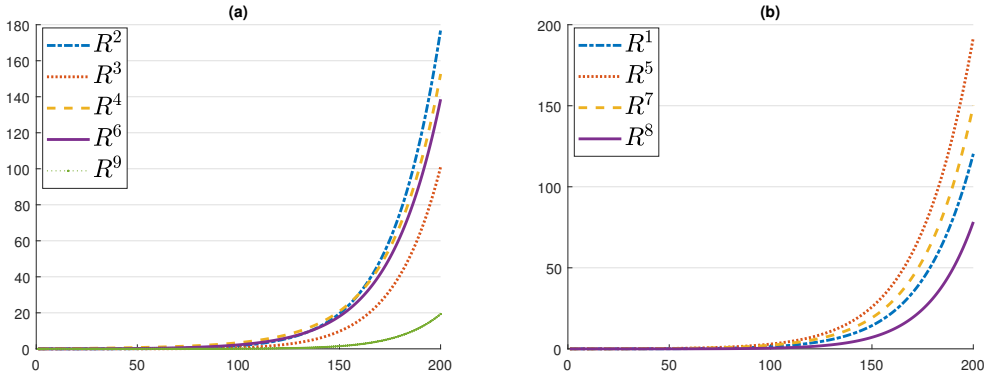

These simulations show the necessity of some interventions to avoid these huge numbers of infections, especially in the epicenter of the epidemic and the surrounding zones.

4.4. Scenario 1: Travel-restriction only where $\mathscr{I}^{\mathscr{T}}{}_{min} = 1000$. Figures 8 and 9 show the number of susceptible people from the 9 regions applying the travel-restriction control strategy from 1000 infected. In all regions, the number of susceptible individuals remains constant throughout the strategy period. On the other hand, for the case without control, the number of susceptible people experienced a slight decrease from the instant $i = 150$ to reach a regression of about 10^4 cases towards the end.

FIGURE 8. Temporal evolution of susceptible populations with only the travel-restriction control where $\mathscr{J}^{\mathscr{T}}{}_{min} = 1000$.

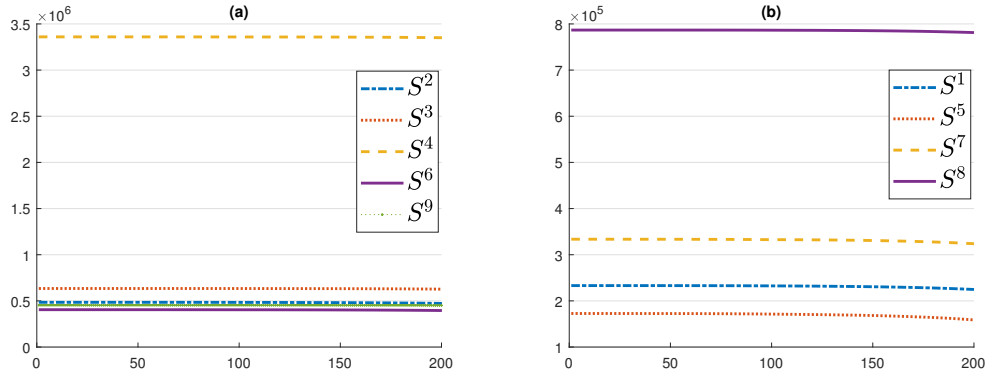

FIGURE 9. Geographical spread of susceptible individuals with only the travel-restriction control where $\mathscr{J}^{\mathscr{T}}{}_{min} = 1000$.

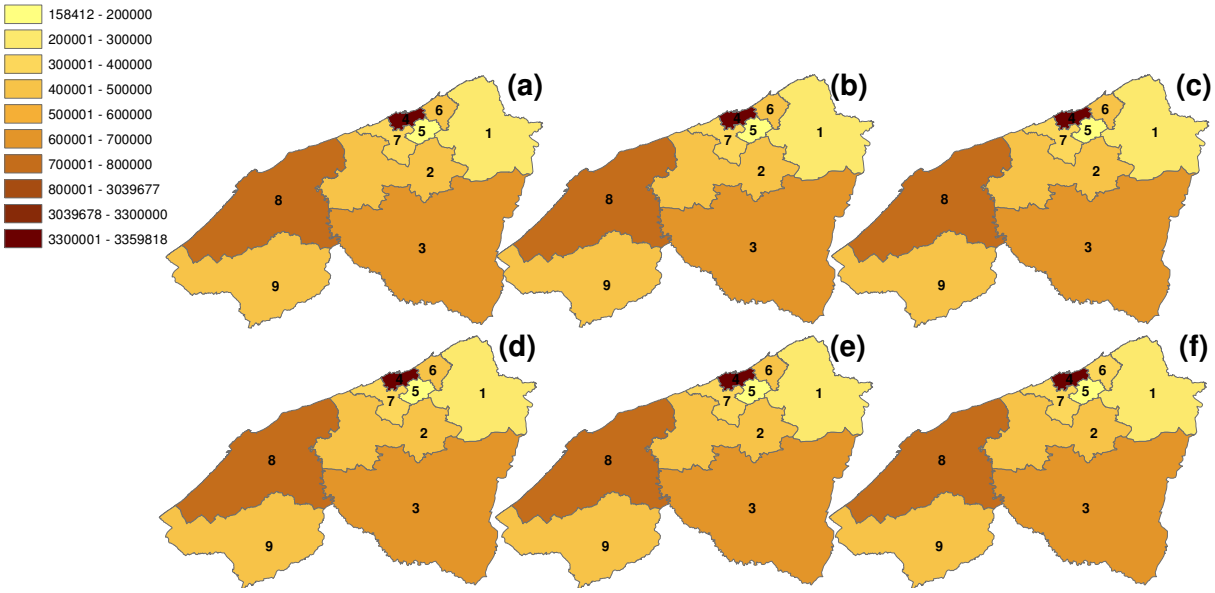

Figures 10 and 11 represent the evolution of the infected by applying the travel-restriction control strategy from 1000 infected in the different regions. We note that at the beginning all the regions register no infected and that from the instant $i = 100$, the number of infected increases rapidly, especially for the regions C_2, C_5, C_6, C_7, which surround the metropolis C_4, and who have reached a maximum value about 14000 infected. The regions C_8, and C_9 recorded, at the moment $i = 200$, a maximum value which is less than 6000 cases. On the other hand, without a

FIGURE 10. Temporal evolution of infected populations with only the travel-restriction control where $\mathscr{J}^{\mathscr{T}}{}_{min} = 1000$.

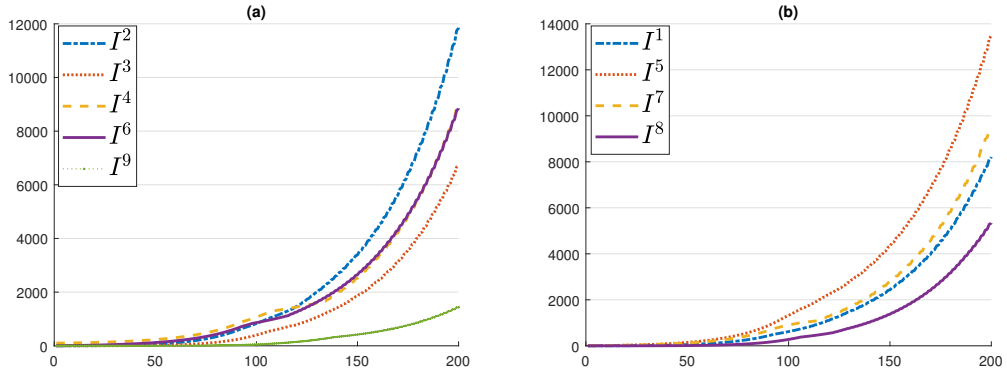

FIGURE 11. Geographical spread of infected individuals with only the travel-restriction control where $\mathscr{J}^{\mathscr{T}}{}_{min} = 1000$.

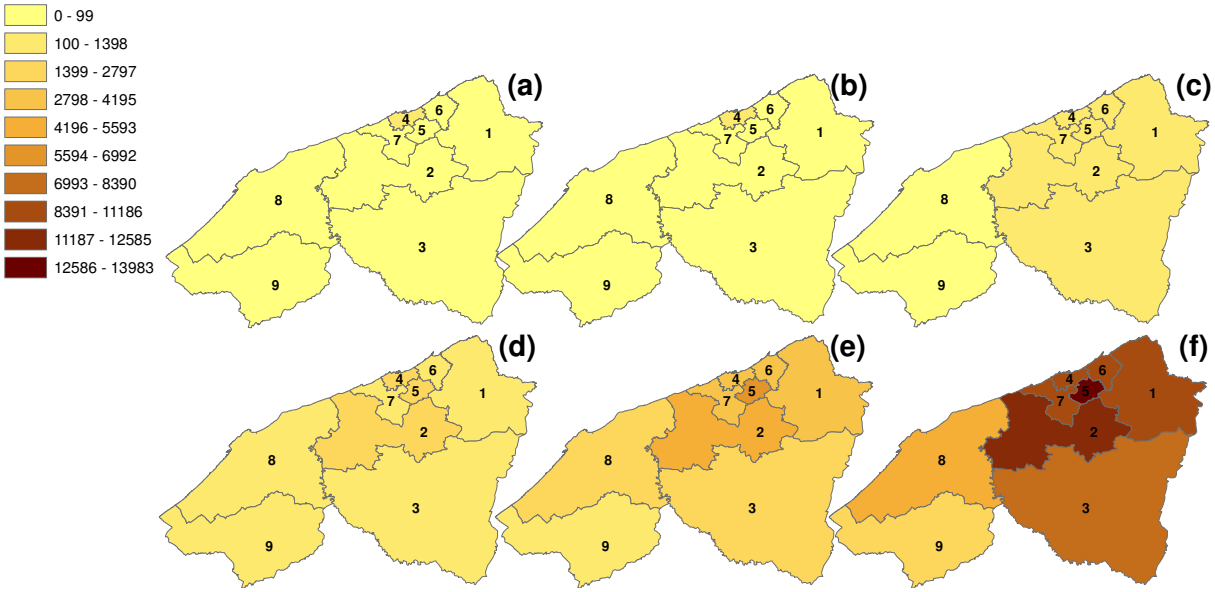

control strategy, the infected began to evolve from the moment $i = 150$ and recorded numbers of infected 6 times more than with the travel-restriction strategy.

Figures 12 and 13 show the evolution of the recovered with the strategy of travel-restriction controls from 1000 infected in the provinces of Casablanca-Settat . It is noted in the regions closest to metropolitan C_4, the numbers of recovered persons began to change from the time $i = 50$. Then the other regions further afield, their numbers of recovered only change from the instant $i = 75$ and gradually increase to reach their maximum values at the end of the controls

FIGURE 12. Temporal evolution of recovered populations with only the travel-restriction control where $\mathscr{I}^{\mathscr{T}}{}_{min} = 1000$.

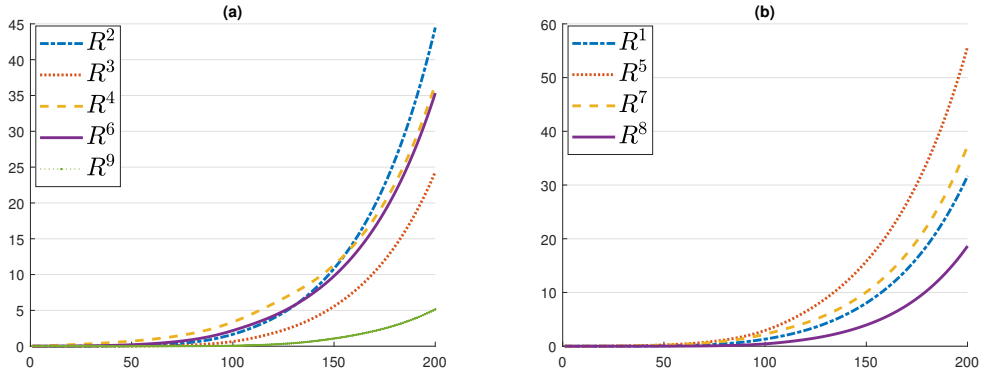

FIGURE 13. Geographical spread of recovered individuals with only the travel-restriction control where $\mathscr{I}^{\mathscr{T}}{}_{min} = 1000$.

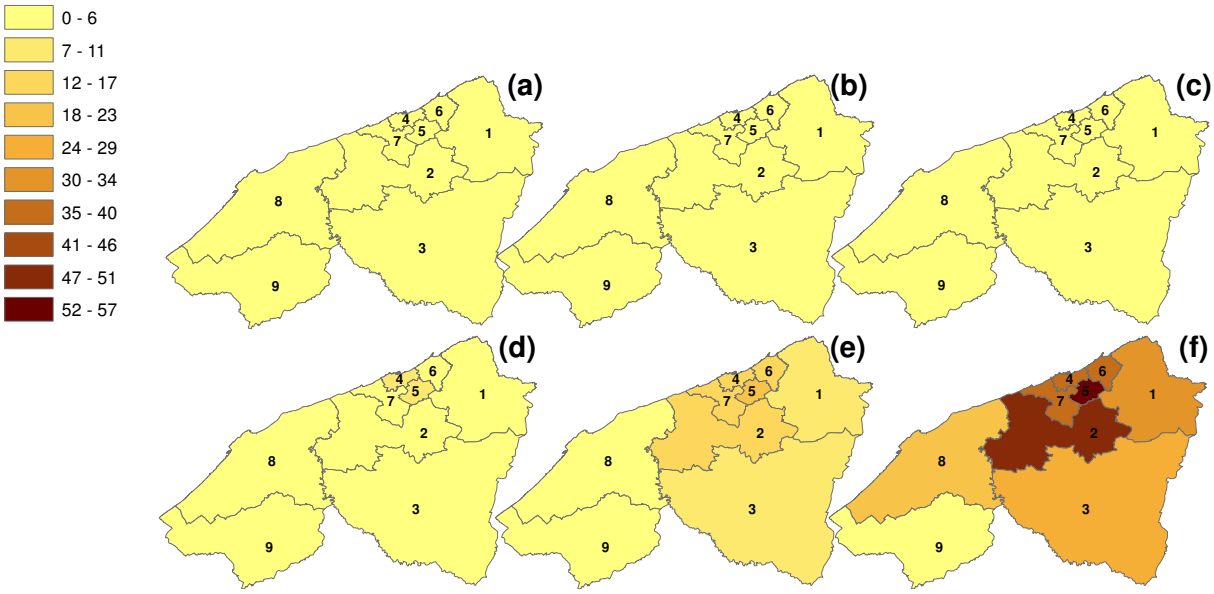

campaign. These numbers of recovered are very low compared to the case without control which does not exceed 55 cases for the regions close to Casablanca and the other regions less than 38 cases and this is due to the fact that the numbers of infected are also low compared to the case without control.

4.5. Scenario 2: Travel-restriction only where $\mathscr{I}^{\mathscr{T}}{}_{min} = 100$. Now, we propose another strategy which consists in defining a travel-restriction on all the provinces from 0 infected i.e by blocking the travel between the regions. This type of strategy is introduced when there is

FIGURE 14. Temporal evolution of susceptible populations with only the travel-restriction control where $\mathscr{I}^{\mathscr{T}}{}_{min} = 100$.

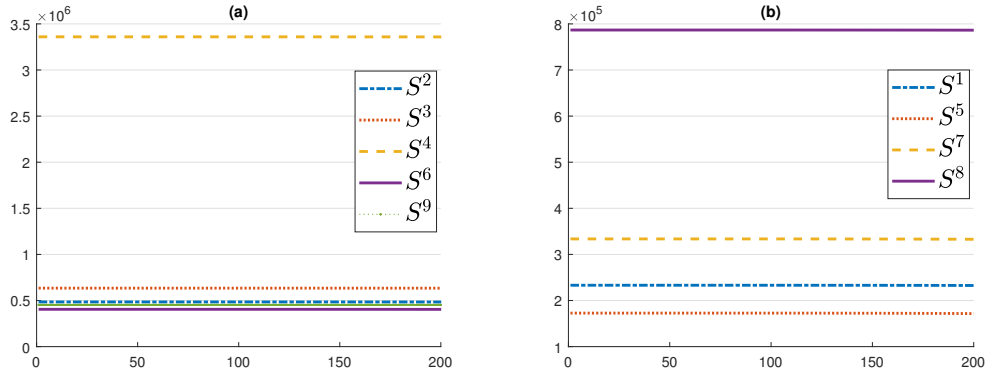

FIGURE 15. Geographical spread of susceptible individuals with only the travel-restriction control where $\mathscr{I}^{\mathscr{T}}{}_{min} = 100$.

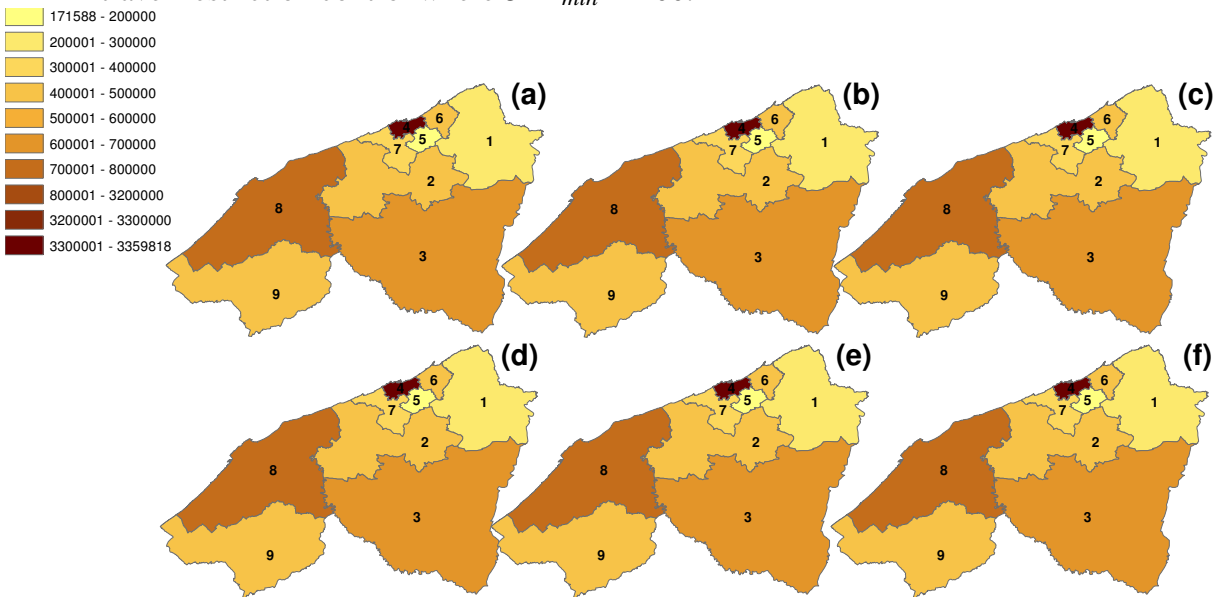

a second wave of the epidemic, when we detect infections in a region and we are aware of the gravity of the virus spread, for example, the case of the Corona-virus pandemics (SARS, MERS, or COVID-19) or Ebola ...

Figures 14 and 15 show the evolution of the numbers of susceptible people in the 9 regions by applying the travel-restriction strategy in all regions from zero infection. We note that throughout the strategy, the number of susceptible remained constant in all 9

regions.

FIGURE 16. Temporal evolution of infected populations with only the travel-restriction control where $\mathscr{I}^{\mathscr{T}}{}_{min} = 100$.

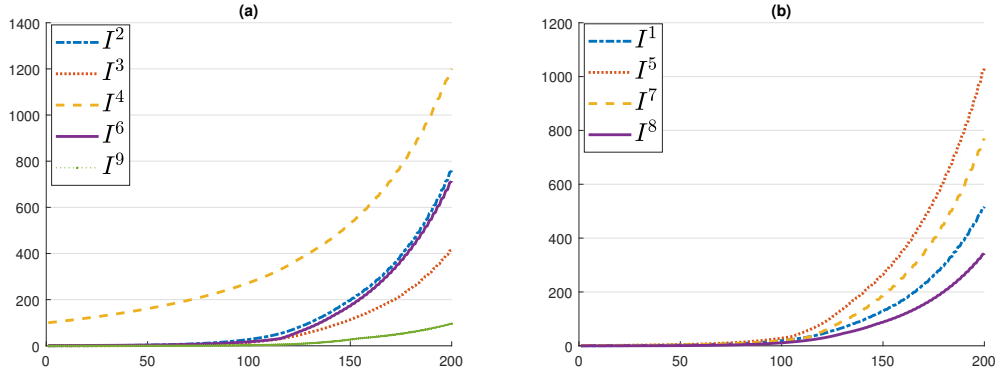

Figures 16 and 17 show the evolution of the numbers of infected in all regions of the provinces of Casablanca-Settat by applying the travel-restriction strategy in all regions, from the appearance of infection in a region and choose blocking trips between regions. In this case, all the regions did not experience any infection throughout the period except the city of Casablanca C_4 which experienced 100 infected at the initial time and this number increased to reach at the moment $i = 200$, 1200 infected. For regions C_5, C_6,C_7 and C_2 only experienced an infection at the time $i = 100$ and from that moment the number of infections increased to reach the maximum number more than 700 cases at the end of the period. So the infected are only limited in the regions close to C_4, on the other hand without control the infected progress exponentially from the instant $i = 100$ and reach values between 10^4 and 10^5 infected.

Like the numbers of infected with travel-restriction strategy from zero infected, all regions display less than 4 recovered throughout the period, except region C_4 which experienced 8 cases of recovered towards the end of the period, as it can be seen from Fig.18 and Fig.19. Since in this strategy the numbers of infected individuals are less important than with the strategy without control.

4.6. Scenario 3: Travel-restriction and vaccination controls where $\mathscr{I}^{\mathscr{T}}{}_{min} = 1000$ and $\mathscr{I}^{\mathscr{V}}{}_{min} = 200$. Figures 20 and 21 show the evolution of susceptible people in the different regions of the provinces of Casablanca-Settat with the application of a vaccination strategy from 200 infected and travel-restriction from 1000 infected. We notice that the susceptible individuals of regions C_1, C_2,C_4 ,C_5, C_6 and C_7 that are closest to Casablanca begins to decrease

FIGURE 17. Geographical spread of infected individuals with only the travel-restriction control where $\mathscr{I}^{\mathscr{T}}{}_{min} = 100$.

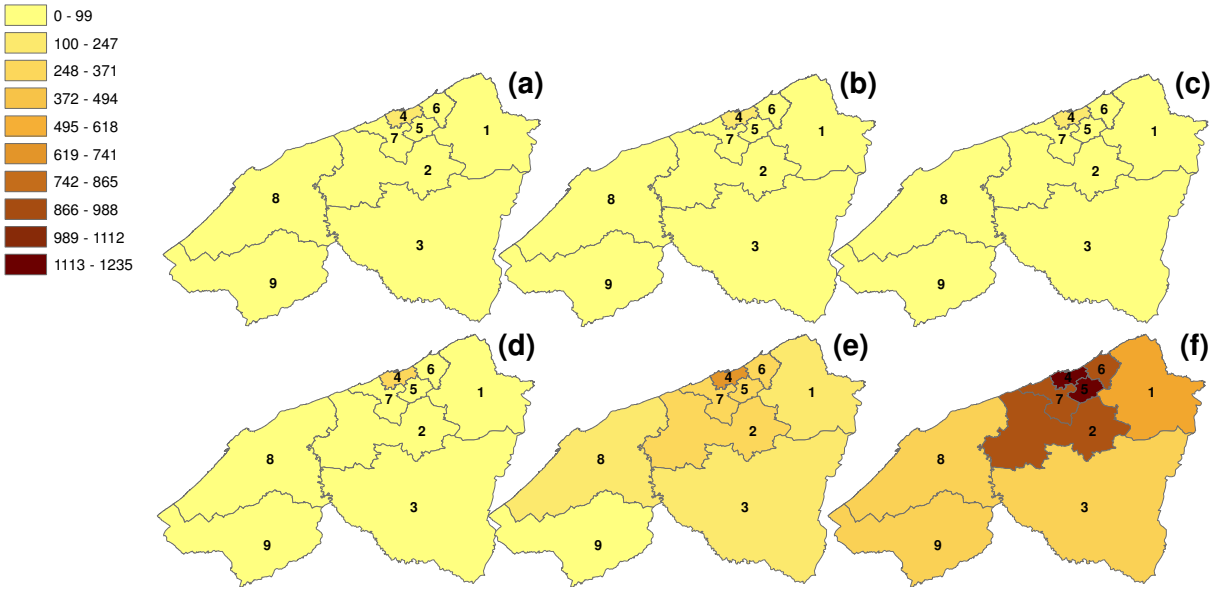

FIGURE 18. Temporal evolution of recovered populations with only the travel-restriction control where $\mathscr{I}^{\mathscr{T}}{}_{min} = 100$.

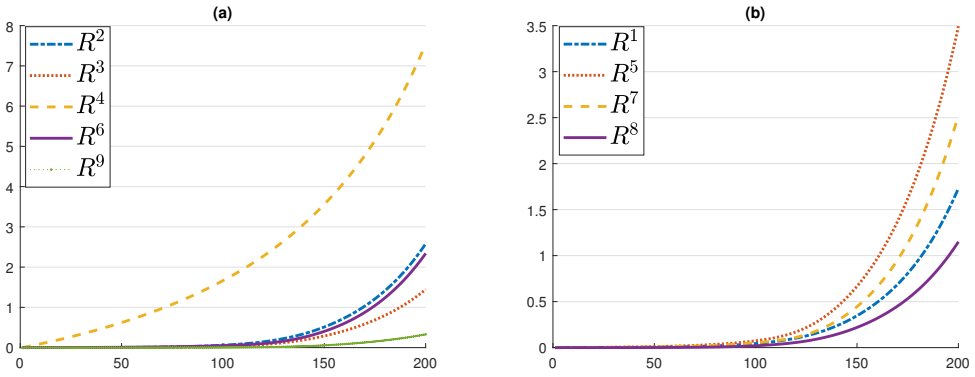

very quickly and reach towards 0 from the moment $i = 80$, then the susceptible of regions C_3 which converges to 0 from the moment $i = 100$ and after those the regions C_8 from $i = 125$ and finally the extreme regions C_9 from the moment $i = 150$. So for this strategy, the numbers of susceptible individuals tend towards 0

Figures 22 and 23 represent the evolution of the infected in the 9 regions by applying the strategy which combines vaccination as soon as the 200 infected appear and travel-restriction from 1000 infected in a region. It is noted that the infected from regions C_1, C_2, C_5, C_7 and C_7

FIGURE 19. Geographical spread of recovered individuals with only the travel-restriction control where $\mathscr{I}^{\mathscr{T}}{}_{min} = 100$.

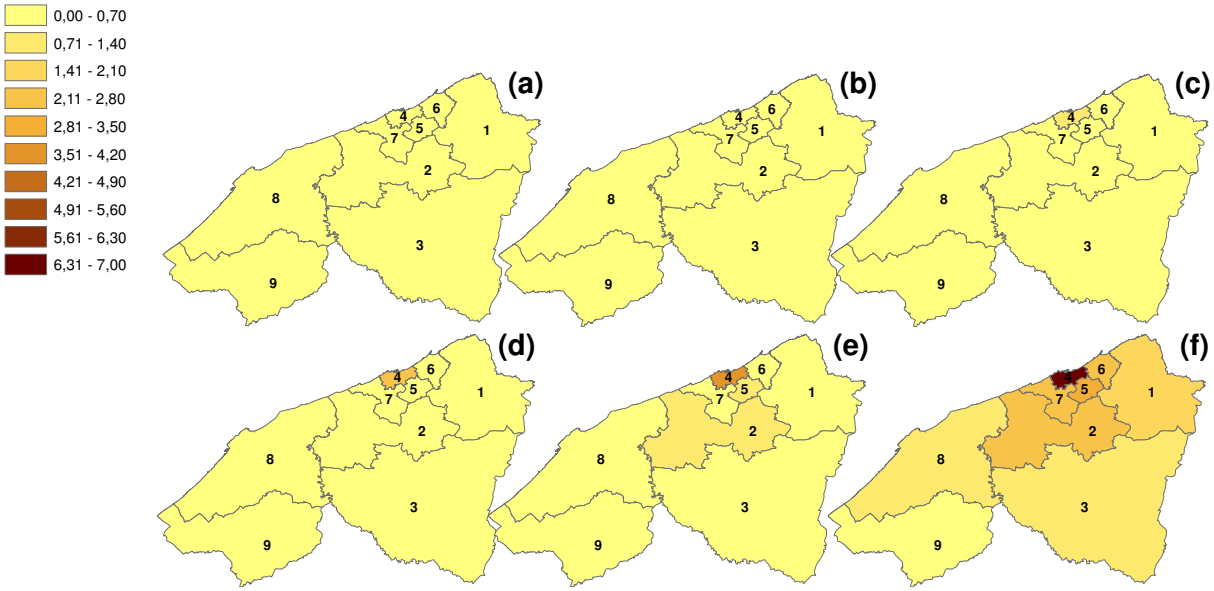

FIGURE 20. Temporal evolution of susceptible populations with the the travel-restriction and vaccination controls where $\mathscr{I}^{\mathscr{T}}{}_{min} = 1000$ and $\mathscr{I}^{\mathscr{V}}{}_{min} = 200$.

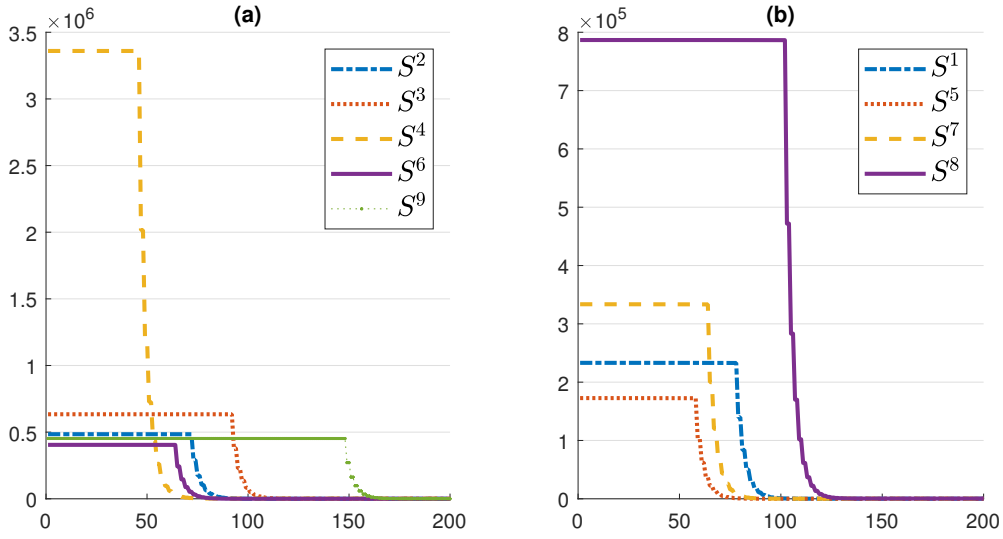

which surround the region of Casablanca, that experienced the appearance of 100 cases infected in the initial state, experienced an increase from the start of the strategy, then the regions C_3, C_6, C_7 which started to grow from the time $i = 25$, . All infected from the 9 regions reach the maximum value of about 250 cases infected at the instant between $i = 75$ and $i = 100$, and remain stagnant until the end of the period. With this strategy, the travel-restriction application

FIGURE 21. Geographical spread of susceptible individuals with the the travel-restriction and vaccination controls where $\mathscr{I}^{\mathscr{T}}{}_{min} = 1000$ and $\mathscr{I}^{\mathscr{V}}{}_{min} = 200$.

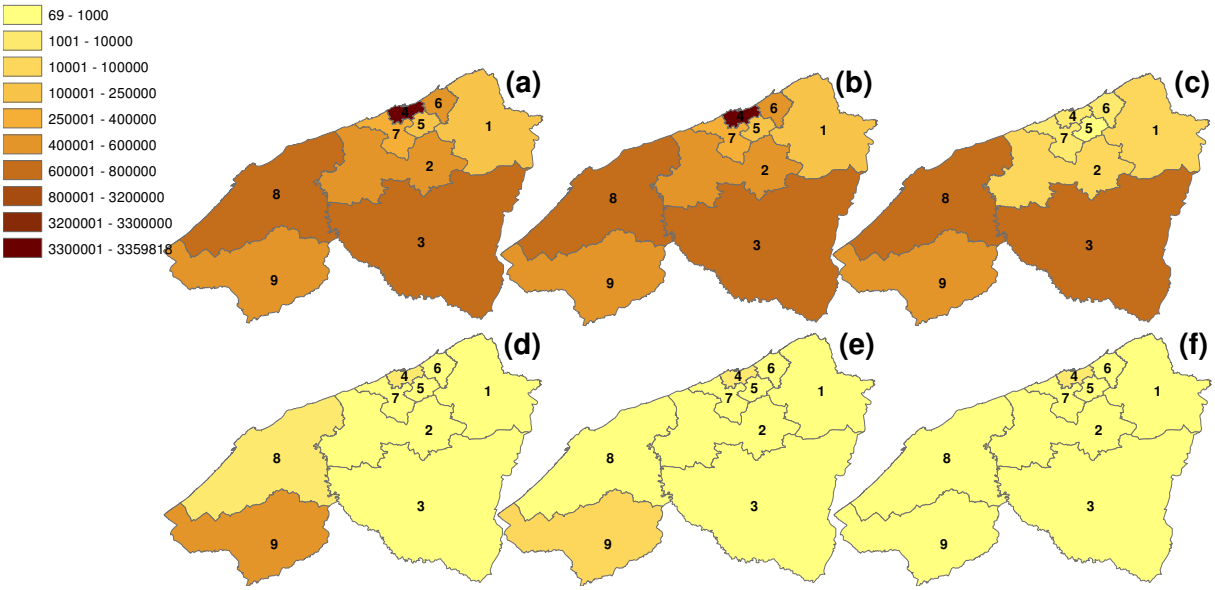

FIGURE 22. Temporal evolution of infected populations with the the travel-restriction and vaccination controls where $\mathscr{I}^{\mathscr{T}}{}_{min} = 1000$ and $\mathscr{I}^{\mathscr{V}}{}_{min} = 200$.

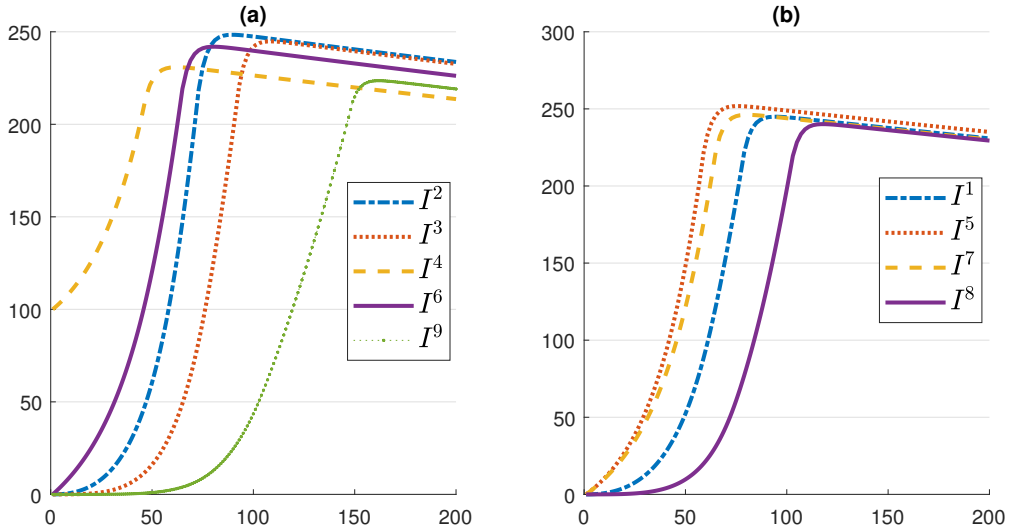

does not applied since the infected not exceed 260 cases. On the other hand, this strategy gives good results compared to without control and also compared to the strategy with travel-restriction at 1000 infected, but less effective than the strategy with travel-restriction at 100 infected.

FIGURE 23. Geographical spread of infected individuals with the the travel-restriction and vaccination controls where $\mathscr{I}^{\mathscr{T}}{}_{min} = 1000$ and $\mathscr{I}^{\mathscr{V}}{}_{min} = 200$.

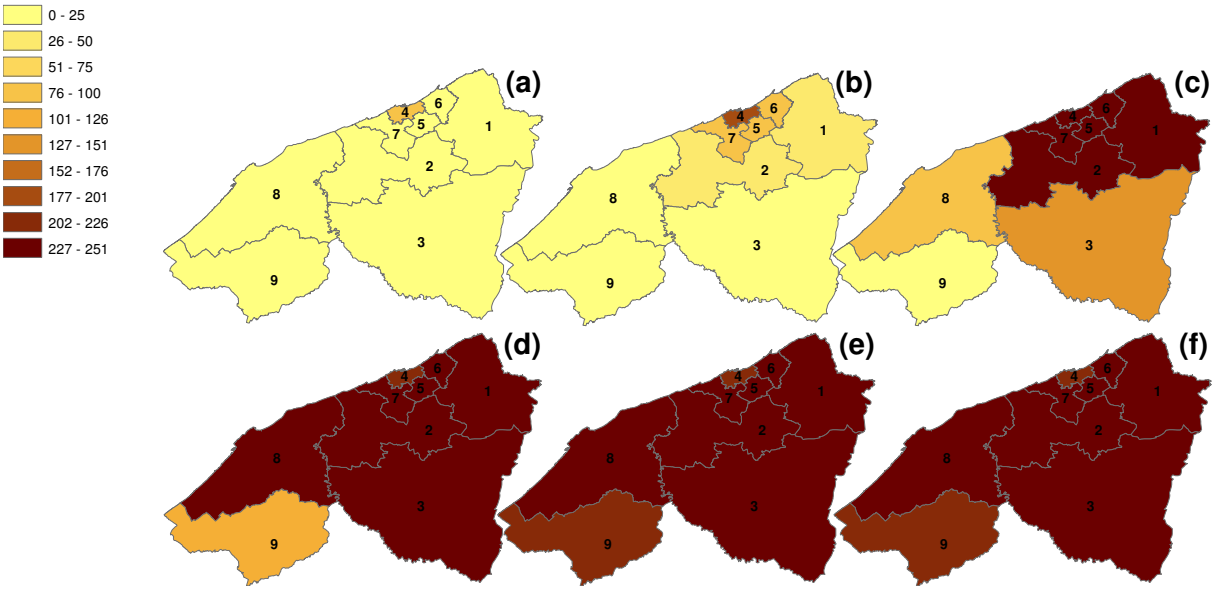

Figures 24 and 25 show the evolution of the recovered in the 9 regions by applying the vaccination strategy from 200 infected and the travel-restriction from 1000 infected. It is noted that the numbers of the recovered people of all the regions believe very quickly, starting from the instants $i = 50$, $i = 75$, $i = 100$ and $i = 150$, with maximum values which vary between 1.5×10^5 and 3.4×10^6. The regions closest to Casablanca begin to grow at the start, then the least close and then the farthest from Casablanca. This strategy gives better results for the recovered than that without control, whose recovered does not exceed 200 cases, or with the strategies with travel-restriction at 100 infected that do not exceed the 7 recovered.

4.7. Scenario 4: Travel-restriction and vaccination controls where $\mathscr{I}^{\mathscr{T}}{}_{min} = 100$ and $\mathscr{I}^{\mathscr{V}}{}_{min} = 200$. Figures 26 and 27 represents the evolution of susceptible people in the different regions of the provinces of Casablanca-Settat with the application of a vaccination strategy from 200 infected and travel-restriction from 100 infected. The evolution of the susceptible is almost the same as that of the strategy with vaccination at 200 infected and travel-restriction at 1000 infected with a slight improvement in convergence time towards 0. We notice that the susceptible of regions C_1, C_2, C_5, C_6 and C_7 that are closest to Casablanca begins to decrease very quickly and reach towards 0 from the moment $i = 150$, then the susceptible of regions C_3,

FIGURE 24. Temporal evolution of recovered populations with the the travel-restriction and vaccination controls where $\mathscr{I}^{\mathscr{T}}{}_{min} = 1000$ and $\mathscr{I}^{\mathscr{V}}{}_{min} = 200$.

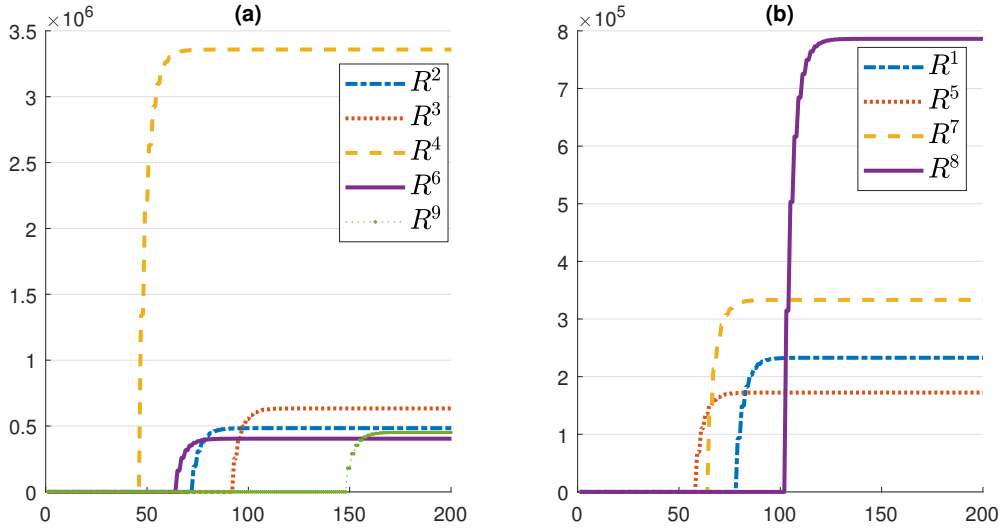

FIGURE 25. Geographical spread of recovered individuals with the the travel-restriction and vaccination controls where $\mathscr{I}^{\mathscr{T}}{}_{min} = 1000$ and $\mathscr{I}^{\mathscr{V}}{}_{min} = 200$.

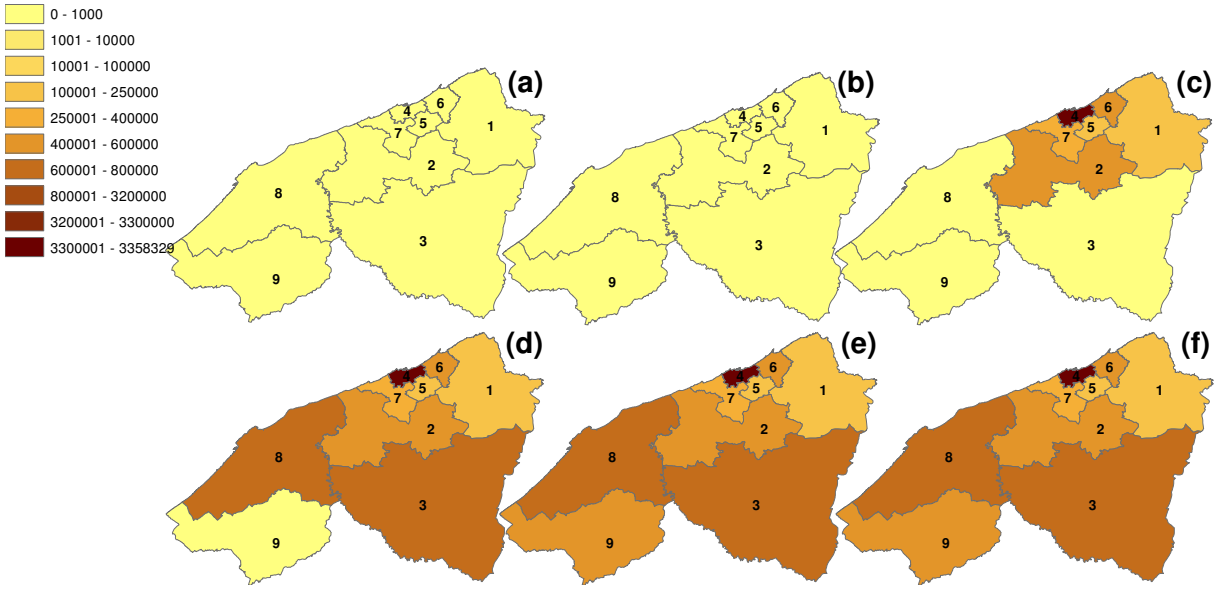

C_8, which converges to 0 from the moment $i = 175$ and after those of the most distant regions C_9 from Casablanca stayed constant until the end . So for this strategy, the numbers of susceptible individuals tend towards 0 from a certain moment, on the other hand for the previous strategies the numbers of susceptible population remain almost constant and decrease slightly from the instant $i = 150$.

FIGURE 26. Temporal evolution of susceptible populations with the the travel-restriction and vaccination controls where $\mathscr{I}^{\mathscr{T}}{}_{min} = 100$ and $\mathscr{I}^{\mathscr{V}}{}_{min} = 200$.

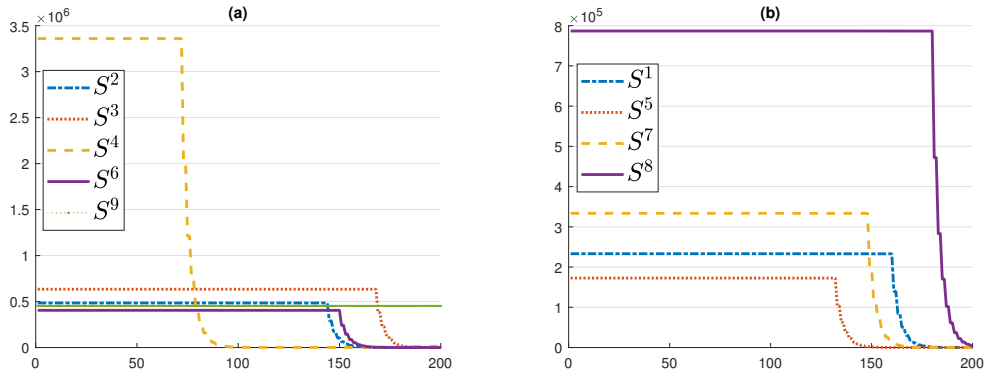

FIGURE 27. Geographical spread of susceptible individuals with the the travel-restriction and vaccination controls where $\mathscr{I}^{\mathscr{T}}{}_{min} = 100$ and $\mathscr{I}^{\mathscr{V}}{}_{min} = 200$.

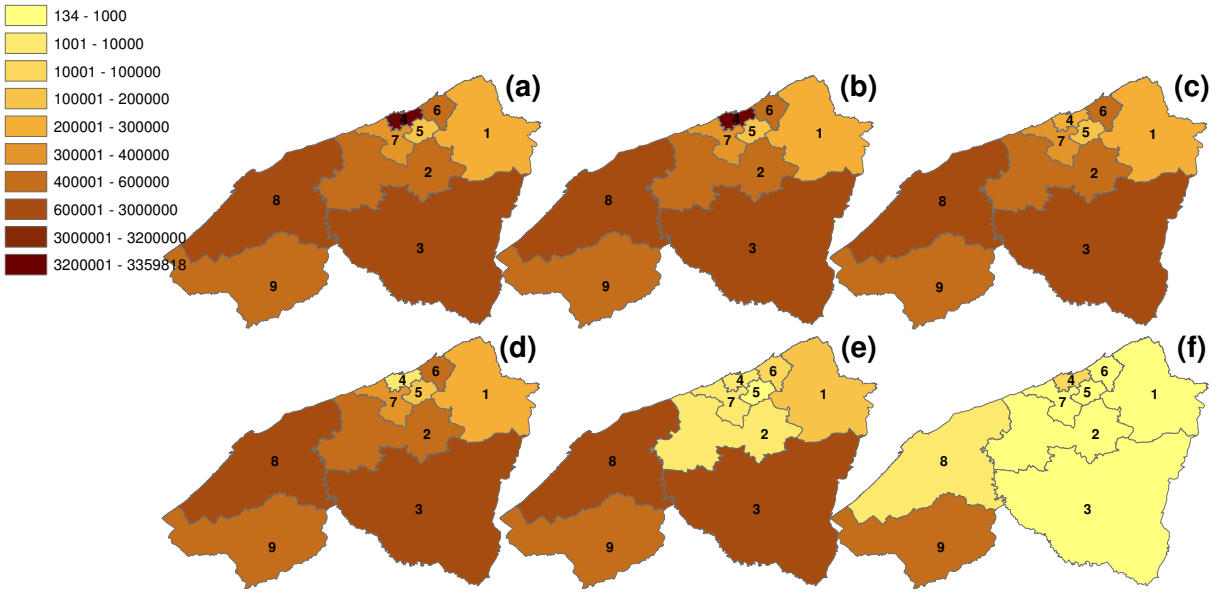

Figures 28 and 29 represent the evolution of the infected in the 9 regions by applying the strategy which combines treatment as soon as the 200 infected appear and travel-restriction from 100 infected in a region. With this strategy, the numbers of infected also remain stagnant from the moment $i = 150$ and do not exceed the value of 250 cases in almost all regions and remain stagnant until the end of the period. We notice a slight improvement compared to the vaccination strategy for 200 infected and travel-restriction for 1000 infected and we can say that it gives almost the same values. It is noted that the infected from regions C_1, C_2, C_5, C_6 and C_7

FIGURE 28. Temporal evolution of infected populations with the the travel-restriction and vaccination controls where $\mathscr{I}^{\mathscr{T}}{}_{min} = 100$ and $\mathscr{I}^{\mathscr{V}}{}_{min} = 200$.

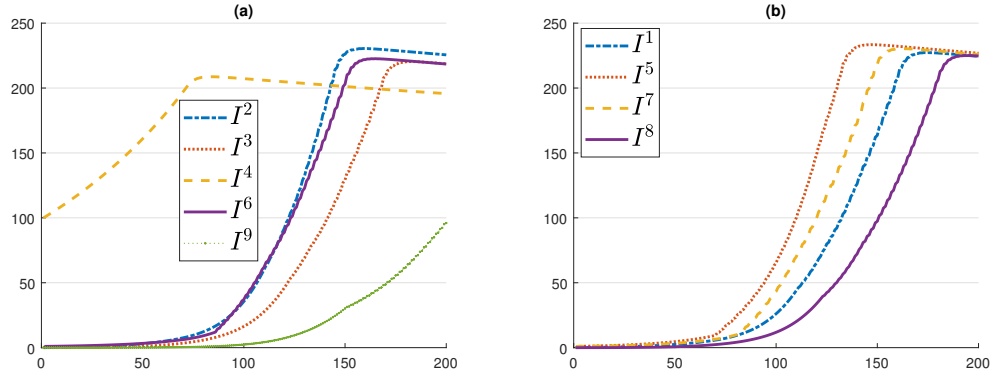

FIGURE 29. Geographical spread of infected individuals with the the travel-restriction and vaccination controls where $\mathscr{I}^{\mathscr{T}}{}_{min} = 100$ and $\mathscr{I}^{\mathscr{V}}{}_{min} = 200$.

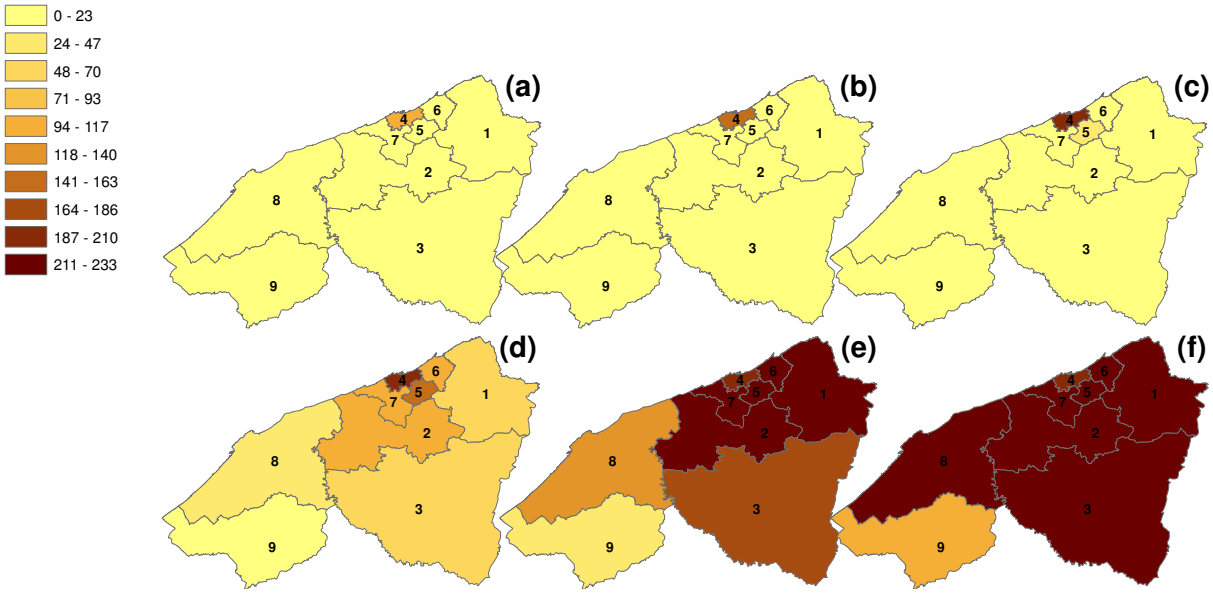

which surround the city of Casablanca C_4, that experienced the appearance of 100 cases infected in the initial state, experienced an increase from the start of the strategy, then the regions C_3, C_8, C_9 which started to grow from the time $i = 50$, then the regions farthest from Casablanca which started to grow at the time $i = 75$. On the other hand, this strategy gives good results compared to without control and also compared to the strategy with travel-restriction at 1000 infected.

Figures 30 and 31 show the evolution of the recovered in the 9 regions by applying the vaccination strategy from 200 infected and the travel-restriction from 100 infected. We notice a

FIGURE 30. Temporal evolution of recovered populations with the the travel-restriction and vaccination controls where $\mathscr{I}^{\mathscr{T}}{}_{min} = 100$ and $\mathscr{I}^{\mathscr{V}}{}_{min} = 200$.

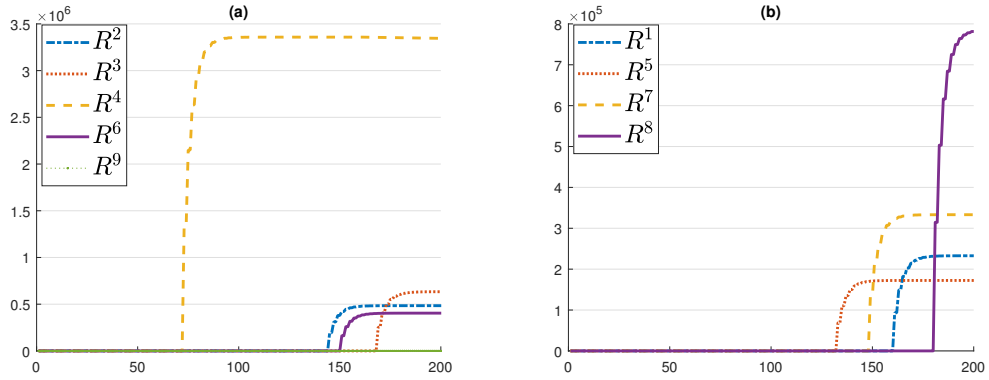

FIGURE 31. $\mathscr{I}^{\mathscr{T}}{}_{min} = 100$ and $\mathscr{I}^{\mathscr{V}}{}_{min} = 200$.

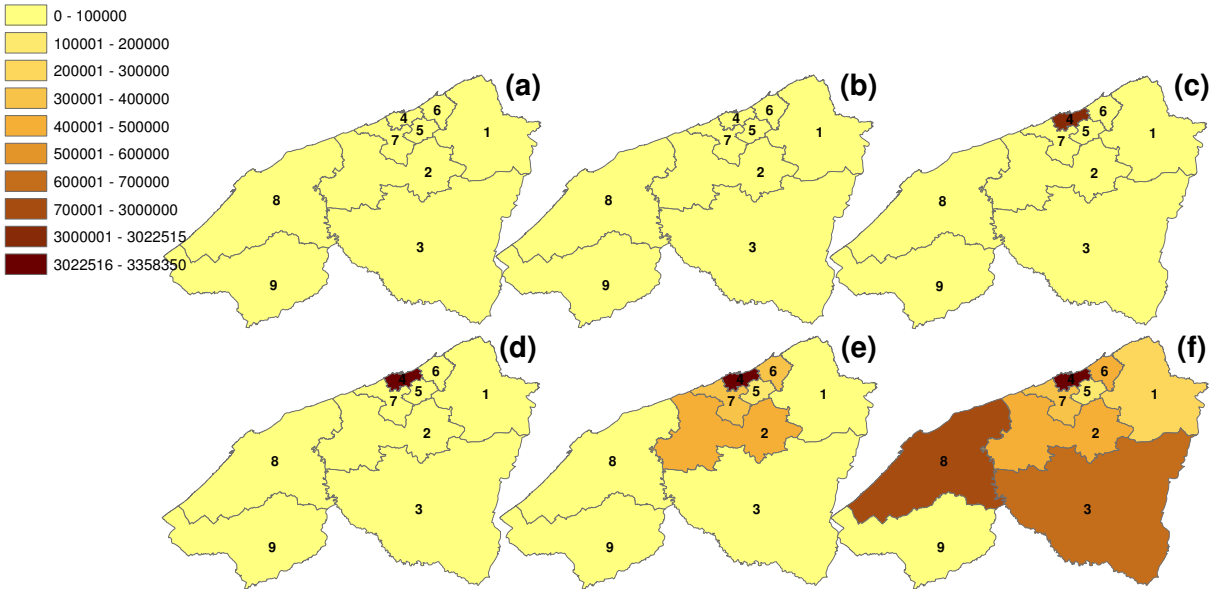

slight improvement compared to the vaccination strategy for 200 infected and travel-restriction for 1000 infected. It is noted that the numbers of the recovered people of all the regions believe very quickly, starting from the instants $i = 75$, $i = 125$, $i = 150$ and $i = 175$, with maximum values which vary between 3.10^5 and 3.10^6. The regions closest to Casablanca begin to grow at the start, then the least close and then the farthest from Casablanca. This strategy gives better results for the recovered than that without control, whose recovered does not exceed 200 cases, or with the strategies with travel-restriction at 100 infected that do not exceed the 7 recovered.

It can be concluded that without a control strategy, the infected explodes and reach extreme values which exceed in almost all regions 10^4 infected. With the travel-restriction strategy from 1000 infected, the number of infected individuals increase in all regions and vary between 1500 and 12000 cases. So there is a decrease compared to cases when there are no controls. With travel-restriction from 100 infected, the numbers of infected do not exceed 800 infected in all regions except the regions C_5 that had maximum values which about 1000 infected and 1200 cases in the region C_4. So with this strategy, the infections are bounded and limited to the regions which surround the metropolitan area C_4. On the other hand, with the vaccination strategy from 200 infections and travel-restriction from 1000 infected individuals, the numbers of infections remain constant with values that do not exceed 250 cases from the moment $i = 100$. With the vaccination strategy from 200 infection and travel-restriction from 100 infection, the numbers of infected individuals also remain stagnant from the moment $i = 100$ and do not exceed the value of 250 cases in almost all regions.

5. CONCLUSION

In this paper, we devised a novel optimization approach that represents a general form of optimal control approaches studied in multi-region framework. We applied this approach to a multi-region discrete epidemic model which has been firstly proposed in [8]. We suggested in this article, a new analysis of infection dynamics in M regions which we supposed to be accessible for health authorities. By defining new importance functions to identify affected areas that must be dealt with, we investigated the effectiveness of optimal vaccination and travel-restriction control approaches, we introduced into the model, control functions associated with appropriate control strategies followed in the targeted regions by mass vaccination campaigns and restrictions and considering different scenarios to compare different strategies. Based on our numerical simulations, we showed the geographical spread of the epidemic and the influence of each region on another and then we deduced the effectiveness of each strategy followed. We concluded that the last scenario of optimal control approach when ${\mathscr{I}^{\mathscr{T}}}_{min} = 100$ and ${\mathscr{I}^{\mathscr{V}}}_{min} = 200$ has given better results than the other cases regarding the maximization of the number of recovered individuals and minimization of the spread of infection in all regions studied.

DATA AVAILABILITY

Data of the actual populations of the Casablanca-Settat region from [26]

CONFLICT OF INTERESTS

The author(s) declare that there is no conflict of interests.

REFERENCES

[1] J. E. Cohen, Mathematics is biology's next microscope, only better; biology is mathematics' next physics, only better, Plos Biol. 2 (12) (2004), e439.

[2] J. D. Murray, Mathematical biology: I. An introduction, Vol. 17, Springer Science & Business Media, 2007.

[3] M. Martcheva, An introduction to mathematical epidemiology, Vol. 61, Springer, 2015.

[4] L. J. Allen, F. Brauer, P. Van den Driessche, J. Wu, Mathematical epidemiology, Vol. 1945, Springer, 2008.

[5] O. Diekmann and J.A.P. Heesterbeek. Mathematical epidemiology of infectious diseases. Wiley, New York, 2000.

[6] H. W. Hethcote, A thousand and one epidemic models, in: Frontiers in mathematical biology, Springer, 1994, pp. 504–515.

[7] H. W. Hethcote, The mathematics of infectious diseases, SIAM Rev. 42 (4) (2000), 599–653.

[8] O. Zakary, M. Rachik, I. Elmouki, On the analysis of a multi-regions discrete sir epidemic model: an optimal control approach, Int. J. Dyn. Control. 5 (3) (2017), 917–930.

[9] W. O. Kermack, A. G. McKendrick, Contributions to the mathematical theory of epidemics i, Bull. Math. Biol. 53 (1-2) (1991), 33–55.

[10] R. Pastor-Satorras, C. Castellano, P. Van Mieghem, A. Vespignani, Epidemic processes in complex networks, Rev. Mod. Phys. 87 (2015), 925–979.

[11] M. I. Meltzer, I. Damon, J. W. LeDuc, J. D. Millar, Modeling potential responses to smallpox as a bioterrorist weapon, Emerg. Infect. Dis. 7 (6) (2001), 959–969.

[12] Y. Zhou, Z. Ma, F. Brauer, A discrete epidemic model for sars transmission and control in china, Math. Comput. Model. 40 (13) (2004), 1491–1506.

[13] R. M. Granich, C. F. Gilks, C. Dye, K. M. De Cock, B. G. Williams, Universal voluntary hiv testing with immediate antiretroviral therapy as a strategy for elimination of hiv transmission: a mathematical model, Lancet. 373 (9657), (2009), 48–57.

[14] Z. Feng, C. Castillo-Chavez, A. F. Capurro, A model for tuberculosis with exogenous reinfection, Theor. Popul. Biol. 57 (3) (2000), 235–247.

[15] V. Capasso, S. Paveri-Fontana, A mathematical model for the 1973 cholera epidemic in the european mediterranean region., Revue d'épidémiologie et de Santé Publiqué 27 (2) (1979), 121–132.

[16] M. Roberts, M. Tobias, Predicting and preventing measles epidemics in new zealand: application of a mathematical model, Epidemiol. Infect. 124 (2) (2000), 279–287.

[17] N. Chitnis, J. M. Cushing, J. Hyman, Bifurcation analysis of a mathematical model for malaria transmission, SIAM J. Appl. Math. 67 (1) (2006), 24–45.

[18] C. C. Mundt, K. E. Sackett, L. D. Wallace, C. Cowger, J. P. Dudley, Aerial dispersal and multiple-scale spread of epidemic disease, EcoHealth 6 (4) (2009), 546–552.

[19] O. Zakary, M. Rachik, I. Elmouki, A multi-regional epidemic model for controlling the spread of ebola: awareness, treatment, and travel-blocking optimal control approaches, Math. Meth. Appl. Sci. 40 (4) (2017), 1265–1279.

[20] O. Zakary, A. Larrache, M. Rachik, I. Elmouki, Effect of awareness programs and travel-blocking operations in the control of hiv/aids outbreaks: a multi-domains sir model, Adv. Differ. Equ. 2016 (2016), 169.

[21] L. S. Pontryagin, Mathematical theory of optimal processes, Routledge, New York, 2018.

[22] Nouveau découpage territorial du royaume? http://www.pncl.gov.ma/fr/News/Alaune/Pages/Nouveau-d%C3%A9coupage-r%C3%A9gional-du-Royaume-.aspx (2015).

[23] What is a shapefile? https://desktop.arcgis.com/en/arcmap/latest/manage-data/shapefiles/what-is-a-shapefile.htm (2020).

[24] what is arcmap?, https://desktop.arcgis.com/fr/arcmap/10.3/main/map/what-is-arcmap-.htm (2020).

[25] An overview of the neighborhood tools, https://desktop.arcgis.com/en/arcmap/10.3/tools/spatial-analyst-toolbox/an-overview-of-the-neighborhood-tools.htm (2020).

[26] Recensement general de la population et de l'habitat 2014, https://www.hcp.ma/reg-casablanca/attachment/673830/ (2015).